Selective Targeting of Homologous Recombination Deficiency

Jutta Zimmer

St Cross College

A thesis submitted to the Division of Medical Sciences at the University of Oxford for the degree of Master of Science by Research

Trinity Term 2014

CRUK and MRC Oxford Institute for Radiation Oncology

Department of Oncology

University of Oxford

Word count: 11,798

CONTENTS

Acknowledgements

Firstly, I thank my supervisor Dr. Madalena Tarsounas for giving me the opportunity to pursue my studies in her laboratory. It has been a very valuable experience to work in her group. She always supported and encouraged me. Thanks to her, I was able to attend my first international meeting and was given many more chances to integrate in the scientific community.

Secondly, I would like to give a special thanks to all lab members: Xianning, Cecilia, Sophie and Eliana. They introduced me to many new techniques and made my days in the lab very enjoyable and productive. Xianning, thank you for the scientific discussions and for proofreading my thesis! Many thanks to Cecilia for teaching me all the tissue culture methods! I thank Sophie for familiarising me with the microscopy techniques.

Thirdly, a special thanks to two members of the CRUK/MRC Oxford Institute for Radiation Oncology, Swagata Halder and Dr. Enni Markkanen. They helped me with the DNA fibre and comet assays, respectively. Thank you both for your contribution!

Lastly, I want to thank my family and friends! A big thanks to my family for their support and confidence in me! My studies and experience in Oxford would not have been possible without them.

Jutta Zimmer St Cross College
Master of Science by Research Trinity Term 2014

Abstract

Homologous recombination (HR) is a key DNA repair pathway essential for cell viability. Counter-intuitively, HR deficiency can trigger carcinogenesis. Understanding the mechanisms that allow the rampant proliferation of HR-deficient tumour cells is crucial for the development of improved therapeutic modalities to selectively inhibit the outgrowth of these cells.

Recently, we identified extracellular signal-regulated kinase 1 (ERK1) as a factor required for the proliferation of BRCA2-deficient cells regardless of their p53 status (Carlos *et al.*, 2013). Here, we report the therapeutic potential of two chemical ERK1/2 inhibitors, SCH772984 and VTX-11e, for selective targeting of HR-deficient tumours due to their ability to specifically obstruct proliferation of HR-deficient cells.

G-quadruplexes (G4s), secondary DNA structures formed by guanine-rich (G-rich) single-stranded DNA (ssDNA), represent natural barriers to replication fork progression. In this study, we demonstrate that treatment with G4 stabilisers selectively decreases viability of BRCA2- and RAD51-deficient cells. We identify DNA damage response activation and acute replication stress as main sources for the cellular toxicity of G4 stabilisers specifically in the context of HR deficiency.

Taken together, the results presented here indicate that HR is required for replication of genomic regions with G4-forming potential to prevent genomic instability stemming from inefficient replication of these sites. Persistent G4 structures lead to DNA damage accumulation, which enables selective killing of cells whose HR-mediated repair has been compromised. This is an important finding with profound implications for the therapeutic exploitation of HR deficiency in the clinic.

Abbreviations

˚C	degree(s) Celsius
53BP1	p53 binding protein 1
ATM	ataxia telangiectasia mutated protein
ATR	ataxia telangiectasia and RAD3-related protein
BLM	Bloom's syndrome protein
BRCA1	breast cancer susceptibility protein 1
BRCA2	breast cancer susceptibility protein 2
cDNA	complementary DNA
CHK1	checkpoint kinase 1
CHK2	checkpoint kinase 2
cm	centimetre(s)
CO_2	carbon dioxide
CtIP	CTBP-interacting protein
DDR	DNA damage response
dH_2O	distilled water
D-loop	displacement loop
DMEM	Dulbecco's modified eagle medium
DMSO	dimethyl sulphoxide
DNA	deoxyribonucleic acid
DNA2	DNA replication helicase 2
DSB	double strand break
DTT	dithiothreitol
DUSP	dual-specificity phosphatase, e.g. DUSP4
ECL	enhanced chemiluminescence
EDTA	ethylene diamine tetraacetic acid
ERK	extracellular signal-regulated kinase
EXO1	exonuclease 1

FACS	fluorescence-activated cell sorting
FBS	fetal bovine serum
FISH	fluorescence *in situ* hybridisation
g	gravity
G-rich	guanine-rich
G4	G-quadruplex
h	hour(s)
HCl	hydrochloric acid
HEK	human embryonic kidney
HR	homologous recombination
HRP	horseradish peroxidase
IB	immunoblotting
IF	immunofluorescence
IgG	immunoglobulin G
Kb	kilo base pair(s)
kDa	kilo Dalton(s)
LB	Luria broth
LT	large T antigen
M	molar
mA	milliampere(s)
MAPK	mitogen-activated protein kinase
mg	milligram(s)
min	minute(s)
mL	millilitre(s)
mM	millimolar
MRE11	meiotic recombination 11
MRN	complex formed by MRE11, RAD50 and NBS1
mRNA	messenger RNA

NBS1	Nijmegen breakage syndrome protein
NHEJ	non-homologous end joining
nm	nanometre(s)
nM	nanomolar
PAGE	polyacrylamide gel electrophoresis
PARP	poly (ADP-ribose) polymerase
PARPi	PARP inhibitor(s)
PBS	phosphate buffered saline
PCR	polymerase chain reaction
RAD	radiation resistance protein, e.g. RAD51, RAD50
RNA	ribonucleic acid
RPA	replication protein A
RT	room temperature
RT-qPCR	real-time quantitative PCR
RTEL	regulator of telomere elongation helicase
s.d.	standard deviation
SDS	sodium dodecyl sulphate
shRNA	small hairpin RNA
siRNA	small interfering RNA
ssDNA	single-stranded DNA
T-loop	telomeric displacement loop
TAE	tris acetate EDTA
Tris	tris (hydroxymethyl) aminomethane
V	Volt
WRN	Werner's syndrome protein
XRCC	X-ray repair complementing defective repair in Chinese hamster cells, e.g. XRCC2
γH2AX	phosphorylated histone 2AX
µ	micro

List of figures

List of Tables

1 Introduction

Cells are constantly at risk of DNA damage giving rise to up to one million DNA lesions per cell per day (Lodish *et al.*, 2004), among which DNA double strand breaks (DSBs) are the most deleterious. Thus, accurate and efficient DNA repair mechanisms are essential to maintain chromosome integrity. Failure of these mechanisms triggers genomic instability, a hallmark of cancer (Negrini *et al.*, 2010), leading to accumulation of DNA damage, chromosome abnormalities, inactivation of tumour suppressor genes and amplification of drug resistance genes. This in turn allows tumours to develop, metastasise and acquire drug resistance. HR is the only error-free repair mechanism that aligns homologous DNA sequences for the reconstitution of the original sequence at DSB sites. The genes engaged in this process are mutated or epigenetically silenced in many cancers enabling genomic instability to drive tumourigenesis.

One other pre-requisite for the maintenance of genome integrity is precise and effective DNA replication. Correct chromosome segregation in mitosis relies on the exact duplication of the entire cellular DNA during the S phase of the cell cycle. Alternative DNA structures such as G4s arise spontaneously during DNA replication and threaten genome stability by obstructing replication fork progression. To prevent loss of genome integrity, known to elicit cell cycle arrest or cancer development, cells have evolved mechanisms that eliminate such structures or promote restart and repair of stalled replication forks.

1.1 G-quadruplexes

G4s are thermodynamically stable secondary structures that G-rich ssDNA can adopt under physiological conditions *in vitro* (Gellert *et al.*, 1962). The signature motif that predicts G4 formation is $G_{3-5}N_{1-3}G_{3-5}N_{1-3}G_{3-5}N_{1-3}G_{3-5}$ (Kruisselbrink *et al.*, 2008). In the human genome, more than 300,000 sites with G4-forming potential have been identified by genome-wide *in silico* analyses (Huppert *et al.*, 2005; Todd *et al.*, 2005). The formation of G4s *in vivo* was first demonstrated by electron microscopy and immunohistochemical studies (Biffi *et al.*, 2013; Duquette *et al.*, 2004). These findings were further supported by isolation of G4 sequences from human genomic DNA and direct visualisation of G4 structures in human cells using G4 ligands and structure-specific antibodies (Lam *et al.*, 2013; Müller *et al.*, 2010).

There is increasing evidence of G4s playing an important role in a variety of biological processes including epigenetic regulation, gene expression, DNA replication initiation and telomere maintenance (Besnard *et al.*, 2012; Sarkies *et al.*, 2012; Sarkies *et al.*, 2010; Smith *et al.*, 2011; Vannier *et al.*, 2012). Paradoxically, G4s also have the potential to cause genomic instability due to their ability to obstruct replication fork progression (Lopes *et al.*, 2011; Paeschke *et al.*, 2011; Ribeyre *et al.*, 2009). A significant characteristic of G4-forming DNA sequences is their recombinogenic and mutagenic potential (Cahoon *et al.*, 2009; Piazza *et al.*, 2010; Ribeyre *et al.*, 2009). Consistent with this notion, enrichment of G4-forming sequences has been implicated in tumour development (De *et al.*, 2011).

Given these negative connotations, it is believed that G4 structures must be resolved during DNA replication in order to preserve genome stability. Various enzymes have been implicated in this process including FANCJ (London *et al.*, 2008;

Sarkies *et al.*, 2012; Wu *et al.*, 2008), RTEL1 (Uringa *et al.*, 2012; Vannier *et al.*, 2012; Vannier *et al.*, 2013), REV1 (Eddy *et al.*, 2014; Sarkies *et al.*, 2010), BLM (Huber *et al.*, 2002; Sun *et al.*, 1998) and WRN (Fry *et al.*, 1999; Mohaghegh *et al.*, 2001). The recently reported remodelling of replication forks stalled at G4 motifs into recombination intermediates (Lopes *et al.*, 2011; Ribeyre *et al.*, 2009) indicates that HR may be required to rescue replication arrest, most likely in conjunction with the enzymatic activities mentioned above.

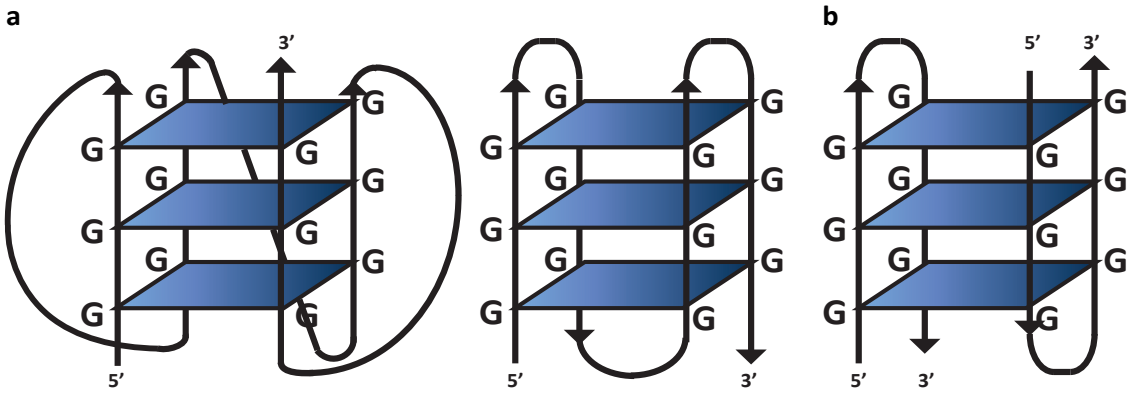

Figure 1: Schematic representation of G4 structures
(**a**) Parallel and antiparallel conformations of intramolecular G4 topologies. (**b**) Two G-rich ssDNA strands dimerised into an intermolecular G4 topology. Adapted from Tarsounas *et al.* (2013).

Telomeres are among the best-characterised sites with G4-forming potential due to their repetitive G-rich DNA sequence (Parkinson *et al.*, 2002). In vertebrates, telomeric DNA is composed of 10-15 Kb of TTAGGG repeats (Denchi *et al.*, 2007; Meyne *et al.*, 1989; Moyzis *et al.*, 1988) ending in a G-rich 3' ssDNA overhang. The main function of these nucleoprotein complexes is to protect chromosome ends from degradation and fusion (McClintock, 1941; Palm *et al.*, 2008). Hence, telomere dysfunction can lead to genomic instability (Blackburn, 2001). HR prevents telomere

fragility by restarting replication forks stalled within the telomeric repeats. Supporting this concept, HR abrogation leads to telomere replication defects and telomere shortening (Badie *et al.*, 2010).

1.2 Homologous recombination in genome integrity

HR is a key mechanism for accurate DSB repair using an intact, homologous sequence as a template (Johnson *et al.*, 2000; Johnson *et al.*, 1999; Valerie *et al.*, 2003). Most commonly, the sister chromatid is the preferred substrate for this error-free repair reaction. Thus, HR mainly operates during S/G2 phase of the cell cycle when a sister chromatid is available (Takata *et al.*, 1998). During DNA replication, HR is required to restart and repair stalled replication forks (Feng *et al.*, 2012; Lomonosov *et al.*, 2003; Nagaraju *et al.*, 2007; Tsang *et al.*, 2008). DNA damage, secondary DNA structures and DNA-bound proteins represent obstacles for replication leading to stalling or collapse of replication forks. HR is the main mechanism for the repair of DSBs arising from disintegrated replication forks (Arnaudeau et al., 2001). Additionally, HR is required to initiate DNA replication (Segurado et al., 2002) as well as to facilitate replication fork progression (Daboussi *et al.*, 2008; Henry-Mowatt *et al.*, 2003).

Recently, it has become clear that HR plays an important role in telomere maintenance by providing a mechanism for telomere elongation (Cesare *et al.*, 2008; Henson *et al.*, 2002) and in telomere capping by facilitating T-loop formation (Verdun *et al.*, 2006).

1.2.1 The HR pathway of DNA repair

Once a DNA DSB occurs, ATM is activated upon recruitment of the MRE11-RAD50-NBS1 (MRN) complex to the DSB site and triggers a downstream DNA damage response (DDR) (Hartlerode *et al.*, 2009; Shiloh, 2003; Shiloh *et al.*, 2013). Factors required to transduce and amplify the DNA damage signal thus generated include the E3 ubiquitin ligases RNF8 and RNF168 as well as MDC1, 53BP1, and BRCA1 (Lukas *et al.*, 2011; Zimmermann *et al.*, 2014). Depending on the phase of the cell cycle (Chapman *et al.*, 2012), DSB ends are either processed into blunt ends that are ligated through non-homologous end joining (NHEJ) repair or resected to generate long 3' ssDNA tails, which represent substrates for HR reactions (Dynan *et al.*, 1998; Heyer *et al.*, 2010). During G1 phase, 53BP1 inhibits end resection thereby promoting DSB repair by NHEJ (Bothmer *et al.*, 2010). To allow end resection and thus repair through HR, BRCA1 competes with and facilitates the removal of 53BP1 in S/G2 phase (Bunting *et al.*, 2010; Chapman *et al.*, 2012).

End resection is initiated by the MRN complex together with CtIP, whilst the BLM helicase and the nucleases DNA2 and EXO1 act to generate the extensive resection required for HR repair (Nimonkar *et al.*, 2011; Nimonkar *et al.*, 2008; Sartori *et al.*, 2007). Other activities are also thought to play a role in resection underlining the key importance of this process in determining the pathway to be engaged in the subsequent repair of the break (Mimitou *et al.*, 2011). RPA binds the resulting ssDNA to protect it from degradation and minimise formation of secondary DNA structures (Chen *et al.*, 2013). This allows BRCA2 and members of the RAD51 paralog family (RAD51B, RAD51C, RAD51D, XRCC2 and XRCC3), the so called recombination mediators, to load the RAD51 recombinase onto the ssDNA and thus displace RPA from

the resected overhangs (Bishop *et al.*, 1998; Johnson *et al.*, 1999; Moynahan *et al.*, 2001; Tarsounas *et al.*, 2004; Yang *et al.*, 2005). The RAD51 recombinase forms helical nucleoprotein filaments (Benson *et al.*, 1994) and triggers strand invasion into an intact, homologous duplex DNA forming a displacement loop, or D-loop (Baumann *et al.*, 1996; Sung, 1994; Sung *et al.*, 1995), thereby initiating the HR reaction that repairs the break. The initial steps of HR together with the key activities required are illustrated in Figure 2.

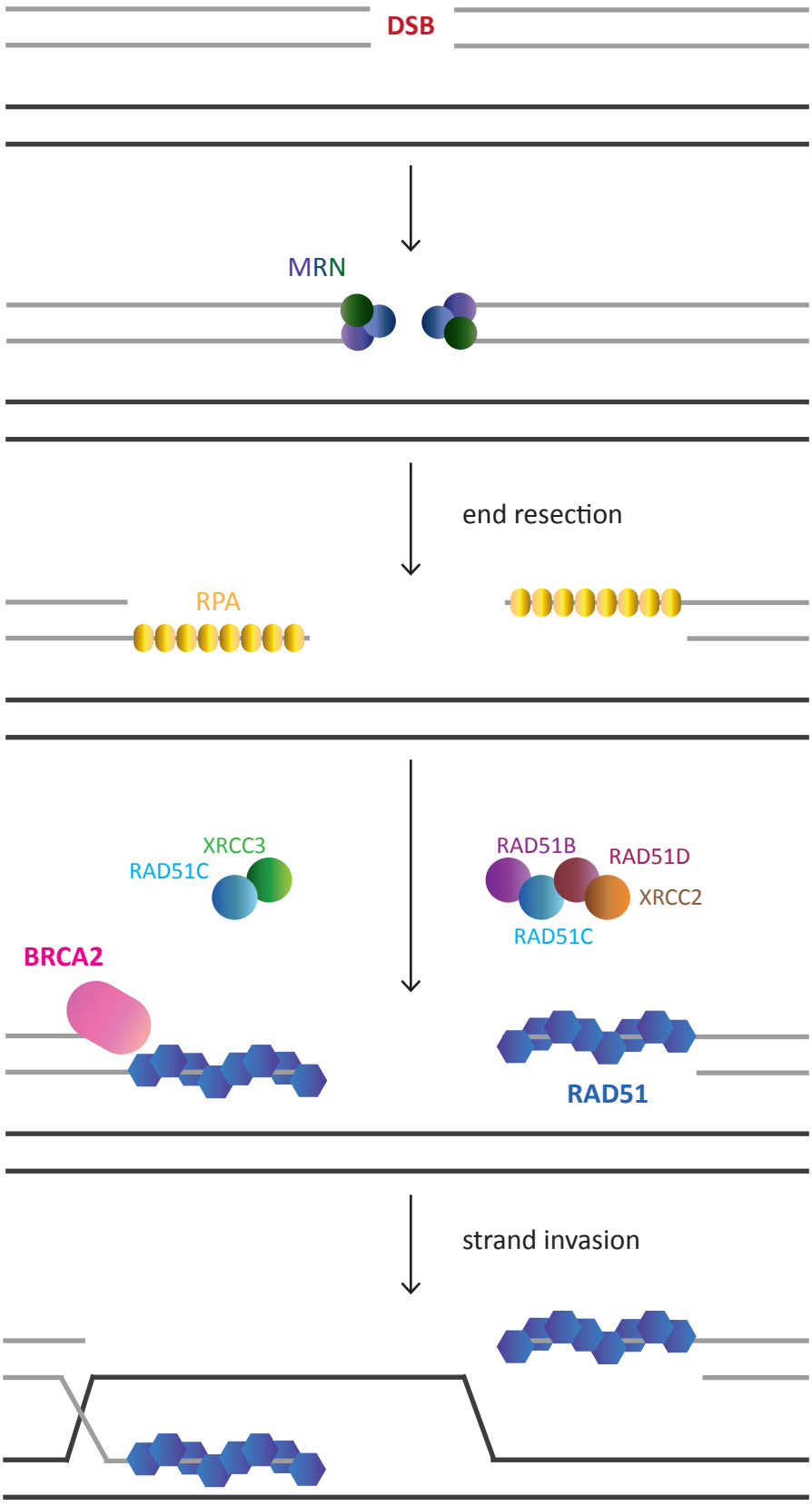

Figure 2: The initiation of the HR pathway of DNA repair in mammalian cells

1.2.2 Consequences of HR abrogation

Chromosome instability is a hallmark of HR-deficient cells leading to checkpoint activation and cell cycle arrest in normal cells (Patel *et al.*, 1998; Xu *et al.*, 1999). Cells with compromised HR capacity fail to preserve genome integrity because they depend on error-prone DSB repair mechanisms, which introduce point mutations or generate translocations through illegitimate chromosome fusions. HR deficiency is associated with hypersensitivity to ionising radiation (Sharan *et al.*, 1997) and DNA-damaging drugs, most of which interfere with replication. For example, aphidicolin inhibits DNA polymerases (Ikegami *et al.*, 1978), hydroxyurea suppresses ribonucleotide reductase (Bianchi *et al.*, 1986) and mitomycin C causes DNA crosslinks, which obstruct replication fork progression (Pan *et al.*, 1986). One of the most prominent examples of chemotherapeutically applied agents is the platinum drug cisplatin, known to induce DNA damage by crosslinking with the purine bases (Dasari *et al.*, 2014).

HR abrogation causes embryonic lethality in mice (Hakem *et al.*, 1996; Suzuki *et al.*, 1997) indicating that HR is essential for viability at cellular and organismal level. Furthermore, defective HR predisposes humans to carcinogenesis (Cerbinskaite *et al.*, 2012). Inactivation of BRCA1 or BRCA2 leads to genome instability (Ban *et al.*, 2001; Gretarsdottir *et al.*, 1998; Tirkkonen *et al.*, 1997; Xu *et al.*, 1999; Yu *et al.*, 2000), a hallmark of cancer (Hanahan *et al.*, 2011; Negrini *et al.*, 2010). Mutations in these tumour suppressor genes are associated with breast and ovarian cancer (King *et al.*, 2003; Rahman *et al.*, 1998; Welcsh *et al.*, 2001). A few years ago, two members of the RAD51 paralog family, *RAD51C* and *RAD51D*, were identified as additional cancer susceptibility genes (Loveday *et al.*, 2012; Meindl *et al.*, 2010; Somyajit *et al.*, 2010).

1.2.3 Mechanisms to sustain proliferation of HR-deficient cells

The fact that HR abrogation can induce tumourigenesis is an apparent contradiction with the cell cycle arrest and cell death it triggers in normal cells (Patel *et al.*, 1998; Xu *et al.*, 1999; Yu *et al.*, 2000). Contrary to *BRCA1*$^{-/-}$ or *BRCA2*$^{-/-}$ primary cells that enter senescence or apoptosis, tumour cells bearing loss-of-function mutations in either *BRCA1* or *BRCA2* genes exhibit an increased proliferative potential. This indicates that the mechanisms that normally prevent cell cycle progression caused by accumulation of excessive, unrepaired DNA damage are abrogated by additional genetic changes. Inactivation of the tumour suppressor gene *TP53* is one prominent example of a mutation that allows survival and growth of tumour cells (Bruchim *et al.*, 2004; Gretarsdottir *et al.*, 1998; Reedy *et al.*, 2001).

In addition to p53 dysfunction, loss of p53 binding protein 1 (53BP1) also reverses the proliferative arrest and embryonic lethality of BRCA1-deficient cells by attenuating the ATM-dependent checkpoint response (Bouwman *et al.*, 2010; Bunting *et al.*, 2010; Cao *et al.*, 2009). On the contrary, survival of BRCA2-defective cells cannot be rescued by depletion of 53BP1 (Bouwman *et al.*, 2010) indicating that distinct signalling pathways sustain the proliferation of BRCA1- and BRCA2-defective tumour cells.

Recently, our laboratory has identified ARF as a factor that plays a crucial role in abolishing proliferation of cells lacking BRCA2 expression (Figure 3). In HR-defective cells, ARF expression is elevated and subsequently induces senescence by stabilising p53 (Carlos *et al.*, 2013). Therefore, ARF functions as a barrier to tumourigenesis in the context of BRCA2 deficiency.

The same study demonstrated that ERK1 is essential for the proliferation of BRCA2-deficient cells in the presence or absence of p53 (Carlos *et al.*, 2013). The latter

is particularly relevant to tumourigenesis, as it is well established that almost all *BRCA2*-deleted human tumours also carry *TP53* mutations. Thus, targeting ERK1 could provide a modality to eliminate BRCA2-deficient cells and tumours in the clinic.

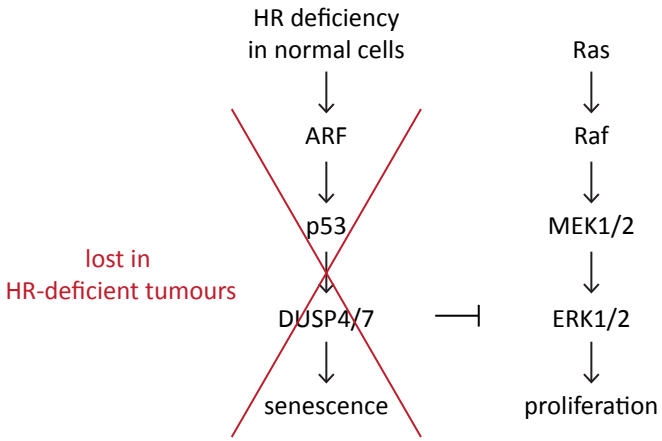

Figure 3: The MAPK pathway allows proliferation of HR-deficient cells
Adapted from Carlos *et al.* (2013) and Chen *et al.* (2001).

The Ras-Raf-MEK1/2-ERK1/2 cascade, also known as the mitogen-activated protein kinase (MAPK) pathway (Figure 3), is a central signalling pathway that regulates fundamental cellular functions and cell proliferation (Chen *et al.*, 2001; Pearson *et al.*, 2001; Xia *et al.*, 1995; Yujiri *et al.*, 1998). Importantly, this pathway is upregulated in almost one third of human tumours (Dhillon *et al.*, 2007), whilst also being essential for the viability of normal cells. Targeting components of the MAPK pathway with chemical compounds has proven clinically unsustainable so far, due to the high toxicity of the inhibitory molecules to normal cells. However, recent inhibitors have been designed that minimise this effect (Morris *et al.*, 2013).

1.2.4 Therapeutic strategies to treat HR-deficient tumours

In the clinic, HR-deficient tumours are often targeted using DNA-damaging radio- and/or chemotherapy. Sensitivity to these treatments relies on the inadequate repair of the DNA damage thus introduced in the absence of HR. Platinum drugs are one example of chemotherapeutic reagents functioning according to this concept (Piccart *et al.*, 2001) and are known to be effective on both, BRCA1- and BRCA2-deficient tumours.

More recently, exploiting synthetic lethality emerged as a promising approach for cancer treatment. According to the concept of synthetic lethality, the combination of defects in multiple individual genes results in cell death, whereas mutation of only one of the genes is compatible with cell viability (Dobzhansky, 1946). Following this approach, poly (ADP-ribose) polymerase (PARP) inhibition was identified as a potent mechanism to specifically kill HR-deficient cancer cells (Bryant *et al.*, 2005; Farmer *et al.*, 2005). In the absence of PARP, persistent ssDNA breaks presumably cause stalled replication forks, which become converted into lethal DSBs in subsequent cell cycles (Lord *et al.*, 2012). In normal cells, this effect can be rescued by restart or repair of stalled replication forks through HR. Recent clinical trials with PARP inhibitors (PARPi) provided encouraging results for effective treatment of tumours associated with HR dysfunction (Audeh *et al.*, 2010; Fong *et al.*, 2009; Tutt *et al.*, 2010).

Acquired clinical resistance to both, platinum drugs and PARPi, is one major drawback in cancer treatment. It appears that the genomic instability characteristic of HR-deficient cancer cells does not only sensitise them to DNA-damaging therapies, but also encourages cells to acquire additional mutations that potentially promote therapy

resistance. For example, rearrangements in *BRCA1/2* genes can reverse the corresponding mutations and lead to synthesis of functional HR proteins thus restoring the capability to repair DNA damage accurately (Barber *et al.*, 2013; Edwards *et al.*, 2008; Sakai *et al.*, 2008). Other mechanisms that mediate PARPi resistance include alteration of an error-prone DNA repair pathway (Chiarugi, 2012; Patel *et al.*, 2011), reduction of PARP levels or activity (Liu *et al.*, 2009) and active elimination of intracellular PARPi (Rottenberg *et al.*, 2008). Nonetheless, the synthetic lethality between ERK1 and BRCA2 using genetic approaches (i.e. shRNA-mediated depletion) raises the possibility that suppressing ERK1 activity chemically may provide effective means to specifically target BRCA2-defective cells and tumours (Carlos *et al.*, 2013).

1.3 Aims of this work

The generic purpose of this study was to identify new therapeutic strategies to selectively target and eliminate HR-deficient mammalian cells. Firstly, we wanted to determine whether chemical inhibition of ERK enzymes could trigger specific killing of HR-deficient cells, similarly to shRNA-mediated ERK inhibition. Secondly, we aimed to assess the effect of G4 stabilisation in the context of HR deficiency. More precisely, we sought to assess cell viability, DNA damage, replication and transcription efficiency after treatment with G4-interacting compounds in HR-proficient and -deficient cells.

2 Materials and methods

2.1 Materials

2.1.1 Cell lines

All cell lines used in this study are listed in Table 1.

Table 1: Cell lines

Cell line	Origin	Supplier
HEK-293T	human embryonic kidney	ATCC
V-C8	derived from the V79 Chinese hamster lung fibroblast cell line	T. Helleday lab
V-C8 (complemented)	derived from the V79 Chinese hamster lung fibroblast cell line, constitutively expressing BRCA2	T. Helleday lab

2.1.2 siRNAs

The sequences of siRNAs used in this study are summarised in Table 2.

Table 2: siRNAs

Name	Sequence	Supplier
hRAD51	CUUUGGCCCACAACCCAUdTdT	Dharmacon
hBRCA2 (Li *et al.*, 2006)	UCAGCUGGCUUCAACUCCAUUdTdT	Dharmacon
AllStars negative control		Qiagen

2.1.3 qPCR primers

Primers used for quantitative PCR (qPCR) are listed in Table 3.

Table 3: qPCR primers

Gene	Name of primers	Supplier
ALAS1	Hs_ALAS1_1_SG QuantiTect Primer Assay	Qiagen
B2M	Hs_B2M_1_SG QuantiTect Primer Assay	Qiagen
MYC	Hs_MYC_1_SG QuantiTect Primer Assay	Qiagen
SRC	Hs_SRC_1_SG QuantiTect Primer Assay	Qiagen
SREBF1	Hs_SREBF1_1_SG QuantiTect Primer Assay	Qiagen

2.1.4 Plasmids

All plasmids used in this study are listed in Table 4.

Table 4: Plasmids

Plasmid	Usage	Supplier
pML113^{PURO}	plasmid-based replication assay	M. Tarsounas lab
10Tel-pML113^{PURO}	plasmid-based replication assay	This study
1KbTel-pML113^{PURO}	plasmid-based replication assay	This study
pBluHCMV	restriction-digested with BamHI and NotI for excision of 1 Kb of telomeric repeats	Dr. E. Gilson

2.1.5 Antibodies

All primary and secondary antibodies used in this study are listed in Table 5 and Table 6, respectively.

Table 5: Primary antibodies

Target, Name	Type	Dilution/Purpose	Target size (kDa)	Supplier
ATM (pS1981), 10H11	mouse anti-human monoclonal IgG	1:1,000 (IB)	350	Cell Signaling
ATM, clone MAT3-4G10/8	mouse anti-human monoclonal IgG	1:5,000 (IB)	350	Sigma-Aldrich
BRCA2, OP95	mouse anti-human monoclonal IgG	1:2,000 (IB)	390	Calbiochem
BRCA2, smB2-9	sheep anti-mouse monoclonal IgG	1:5,000 (IB)	460	Dr. H. Lee
BrdU/ CldU	rat anti-human monoclonal IgG	1: 500 (DNA fibre)		Abcam
BrdU/ IdU	mouse anti-human monoclonal IgG	1: 100 (DNA fibre)		Beckton Dickinson
CHK1 (pS317+pS345)	rabbit anti-human polyclonal IgG	1:1,000 (IB)	56	Cell Signaling
CHK1, sc-8408	mouse anti-human monoclonal IgG	1:1,000 (IB)	54	Santa Cruz
CHK2 (pT68)	rabbit anti-human polyclonal IgG	1:1000 (IB)	62	Cell Signaling
CHK2, clone 7	mouse anti-human monoclonal IgG	1:5,000 (IB)	60	Merck Millipore
cleaved PARP (Asp214)	rabbit anti-human polyclonal IgG	1:2,000 (IB)	89	Cell Signaling
GAPDH, 6C5	mouse anti-human monoclonal IgG	1:30,000 (IB)	37	Novus Biologicals
H2AX, DR1016	rabbit anti-human polyclonal IgG	1:5,000 (IB)	13	Calbiochem
Tubulin, TAT-1	mouse anti-human monoclonal IgG	1:20,000 (IB)	55	CR-UK, Monocolonal Antibody Facility
PARP	rabbit anti-human polyclonal IgG	1:2,000 (IB)	116	Cell Signaling
RAD51, H-92	rabbit anti-human polyclonal IgG	1:2,000 (IB)	37	Santa Cruz Biotechnology
RPA, SWE34	rabbit anti-human polyclonal IgG	1:1,000 (IF)	30	Dr. S. West

Table 5: Primary antibodies (continued)

Target, Name	Type	Dilution	Target size (kDa)	Supplier
RPA2	rat anti-human monoclonal IgG	1:500 (IF)	30	Dr. H.-P. Nasheuer
RPA32 (pS4+pS8)	rabbit anti-human polyclonal IgG	1:4,000 (IB)	32	Bethyl Laboratories
SMC1, BL308	rabbit anti-human polyclonal IgG	1:4,000 (IB)	160	Bethyl Laboratories
γH2AX (S139), clone JBW301	mouse anti-human monoclonal IgG	1:4,000 (IB), 1:2,000 (IF)	15	Merck Millipore

Table 6: Secondary antibodies

Name	Type	Supplier
DAR Cy3	Cy3 donkey anti-rat IgG	Jackson Immuno Research
DAS	donkey anti-sheep IgG-HRP	Santa Cruz
GAM	goat anti-mouse polyclonal IgG-HRP	Dako
GAM Alexa 488	Alexa Fluor 488 goat anti-mouse IgG	Life Technologies
GAR	goat anti-rabbit polyclonal IgG-HRP	Dako
GAR Alexa 488	Alexa Fluor 488 goat anti-rabbit IgG	Life Technologies
RAR	rabbit anti-rat polyclonal IgG-HRP	Dako

2.1.6 Reagents

Laboratory reagents used in this study are compiled in Table 7.

Table 7: Laboratory reagents

Reagent	Supplier
4', 6-diamidino-2-phenylindole (DAPI)	Sigma-Aldrich
5-chloro-2'-deoxyuridine (CldU)	Sigma-Aldrich
5-iodo-2'-deoxyuridine (IdU)	Sigma-Aldrich
1 Kb plus DNA ladder	Invitrogen

Table 7: Laboratory reagents (continued)

Reagent	Supplier
Acetic acid	VWR
Alkaline Phosphatase, Calf Intestinal (CIP)	New England Biolabs
Ampicillin	Fisher Scientific
Antifade Gold	Invitrogen
Blocking reagent	Roche
Bovine serum albumin (BSA)	Sigma-Aldrich
Bromophenol blue	Sigma-Aldrich
Citric acid	Sigma-Aldrich
Cy3-Tel-PNA probe	Applied Biosystems
Deionised formamide	Chemicon Int.
DharmaFECT	Dharmacon
Dimethyl sulphoxide (DMSO)	Sigma-Aldrich
Dithiothreitol (DTT)	Fisher Scientific
DNA Polymerase I, large (Klenow) fragment	New England Biolabs
Dried skimmed milk	Marvel
Dulbecco's modified eagle medium (DMEM)	Sigma-Aldrich
ECL western blotting detection reagents	Thermo Scientific, Merck Millipore, GE Healthcare
Ethanol	Fisher Scientific
Ethidium bromide	Sigma-Aldrich
Ethylene diamine tetraacetic acid (EDTA)	VWR
Fetal bovine serum (FBS)	Life Technologies
Formaldehyde	Merck
Formamide	Sigma-Aldrich
Fuji medical X-ray films	Fuji
Glycerol	Sigma-Aldrich
Goat serum	Sigma-Aldrich
HiMark pre-stained protein standard	Invitrogen

Table 7: Laboratory reagents (continued)

Reagent	Supplier
Hydrochloric acid (HCl)	VWR
Isopropanol	VWR
JetPRIME	Polyplus
Karyo MAX colcemid solution	Life Technologies
LB agar	Sigma-Aldrich
Low-melting agarose	Bio-Rad
Luria broth (LB)	Invitrogen
Magnesium chloride ($MgCl_2$)	Sigma-Aldrich
Maleic acid	Sigma-Aldrich
Methanol	Fisher Scientific
NEB stable competent *Escherichia coli*	New England Biolabs
NuPAGE 10% Bis-Tris gel	Invitrogen
NuPAGE 3-8% Tris-Acetate gel	Invitrogen
NuPAGE MOPS SDS running buffer (20x)	Invitrogen
NuPAGE transfer buffer (20x)	Invitrogen
NuPAGE Tris-Acetate SDS running buffer (20x)	Invitrogen
Olaparib	Stratech
Opti-MEM reduced serum media	Thermo Scientific
PageRuler pre-stained protein ladder	Thermo Scientific
Paraformaldehyde	Electron Microscopy Sciences
Penicillin-streptomycin	Sigma-Aldrich
Pepsin	Sigma-Aldrich
$PhenDC_3$	Dr. M.-P. Teulade-Fichou
Phosphate buffered saline (PBS) tablets (Oxoid)	Fisher Scientific
Photoflo	Kodak

Table 7: Laboratory reagents (continued)

Reagent	Supplier
Power SYBR Green Cells-to-CT kit	Life Technologies
Propidium iodide	Sigma-Aldrich
Proteinase K	Sigma-Aldrich
Puromycin	Sigma-Aldrich
Pyridostatin	Sigma-Aldrich
QIAfiler plasmid maxi kit	Qiagen
QIAprep spin miniprep kit	Qiagen
QIAquick gel extraction kit	Qiagen
QIAquick PCR purification kit	Qiagen
Rapid DNA ligation kit	Roche
Resazurin	Sigma-Aldrich
Restriction enzymes	New England Biolabs
RNase A	Qiagen
SCH772984	Dr. S. Knapp
SlowFade Antifade kit	Molecular Probes
Sodium azide	Sigma-Aldrich
Sodium chloride (NaCl)	Sigma-Aldrich
Sodium citrate	Fisher Scientific
Sodium dodecyl sulphate (SDS)	Fisher Scientific
Sodium hydroxide (NaOH)	VWR
SYBR Gold	Invitrogen
TMPyP4	Calbiochem
Tris	Fisher Scientific
Triton X-100	Sigma-Aldrich
Trypsin-EDTA (1x)	Sigma-Aldrich
Tween 20	Fisher Scientific
UltraPure agarose	Invitrogen

Table 7: Laboratory reagents (continued)

Reagent	Supplier
Vectashield mounting medium	Vector Laboratories
VTX-11e	Dr. S. Knapp
Xylene cyanol FF	Sigma-Aldrich

2.1.7 Instrumentation

Instruments used in this study are listed in Table 8.

Table 8: Instrumentation

Instrument	Type	Supplier
Balance	PL602-S	Mettler Toledo
Cell analyser	FACScan	BD Biosciences
Centrifuge	5424	Eppendorf
Centrifuge	5804R	Eppendorf
Centrifuge	Avanti J-26XP	Beckman Coulter
Centrifuge	Galaxy Mini	VWR
Developer	Compact X4	Xograph
Digital camera	DFC350 FX R2	Leica
Homogeniser	300 V/T Ultrasonic homogeniser	Biologics
Incubator		Binder
Incubator	Galaxy 170R	New Brunswick
Incubator shaker	Innova 44	New Brunswick
Inverted microscope	DMI6000B	Leica
pH meter	SevenEasy	Mettler Toledo
Plate reader	POLARstar Omega	BMG Labtech
Protein gel system	XCell SureLock Mini-Cell	Invitrogen
Shaker	Belly Dancer	Stovall

Table 8: Instrumentation (continued)

Instrument	Type	Supplier
Spectrophotometer	NanoDrop ND-100	Labtech
Thermal cycler	Veriti	Applied Biosystems
Thermal cycler	StepOnePlus Real-Time PCR System	Applied Biosystems
Thermo mixer	5436	Eppendorf
Transilluminator		Fotodyne
Vortex mixer	Vortex-Genie 2	Scientific Industries
Water bath		Fisher Scientific
Western blot transfer unit	XCell II Blot Module	Invitrogen

2.1.8 Software

All software used in this study is listed in Table 9.

Table 9: Software

Name	Version	Supplier
4Peaks	1.7.1	Mek&Tosj
CellQuest Pro		BD Biosciences
Illustrator	CS6	Adobe
ImageJ	1.47v	National Health Institute, USA
Komet	5.5	Andor Technology
LAS-AF		Leica
ModFit LT	4	Verity Software House
Omega	2.10	BMG Labtech
Photoshop	CS3	Adobe
Prism	6.0e	GraphPad Software

Table 9: Software (continued)

Name	Version	Supplier
Serial Cloner	2-6-1	Serial Basics
StepOne software	v2.3	Applied Biosystems

2.2 Methods

2.2.1 Cell culture

All cell lines used in this study were adherent and cultivated as monolayers at 37˚C in 5% CO_2. HEK-293T and V-C8 cell lines were grown in DMEM supplemented with 10% (v/v) FBS and 1% (v/v) penicillin-streptomycin. Cells were sub-cultured when they reached 70-80% confluence. To detach cells for passaging, cells were washed with PBS and incubated with Trypsin-EDTA at 37˚C for 5 minutes (min). Fresh media containing serum was added to neutralise trypsinisation. The number of cells was determined using a haemocytometer.

2.2.2 RNAi transfection

1.5 x 10^6 HEK-293T cells were reverse-transfected with siRNA in a 10 cm dish. Firstly, 5 µL of DharmaFECT reagent was added to 0.5 mL of Opti-MEM reduced serum media and incubated at room temperature (RT) for 5 min. Secondly, this solution was mixed with 0.5 mL Opti-MEM reduced serum media containing 40 nM final concentration of siRNA. This mix was incubated at RT for 20 min and then added to the cell suspension before plating. The media were replaced after 24 hours (h) of incubation at 37˚C. Depletion of the proteins of interest was usually complete 24 h after transfection, as determined using immunoblotting.

2.2.3 Drug treatment

To test the effect of various drugs used in this study, cells were seeded into the wells of a 96-well cell culture plate at densities of 2,500 cells per well. Cells were allowed to attach by incubation at 37˚C for at least 4 h before the growth media were replaced with drug-containing media. Incubation in the presence of the drug continued for up to six days. The media was replaced on the third day of treatment with fresh media containing drug. When HEK-293T cells were concomitantly treated with siRNA, cells were reverse-transfected one day before seeding into 96-well plates. The transfection was repeated every three days after the first transfection.

The drugs used in this study and solvents used to prepare the dilutions indicated in each figure were: olaparib (Stratech) solubilised in DMSO, SCH772984 (a gift from Dr. S. Knapp, University of Oxford) solubilised in DMSO, VTX-11e (a gift from Dr. S. Knapp, University of Oxford) solubilised in DMSO, $PhenDC_3$ (a gift from Dr. M.-P. Teulade-Fichou, Institut Curie Paris) solubilised in DMSO and Pyridostatin (Sigma-Aldrich) solubilised in dH_20.

2.2.4 Cell viability and proliferation assays

To assess cell viability and proliferation, normal growth media were replaced with fresh media containing 10 µg/mL resazurin (Sigma-Aldrich) supplemented with the drugs used for individual treatments followed by incubation at 37˚C for 2 h. Subsequently, fluorescence was measured using a plate reader with the excitation filter set to 544 nm, the emission filter to 590-10 nm and the gain to 1000. After the measurement, the resazurin solution was replaced with fresh drug-containing media if continued cell growth was required. Data were analysed using the Prism software.

2.2.5 Fluorescence-activated cell sorting (FACS)

Cells were harvested by trypsinisation and centrifugation for 10 min at 300x g. The supernatant was removed, and cells were washed in PBS and fixed in 70% (v/v) ice-cold ethanol overnight at 4°C. Fixed cells were pelleted by centrifugation for 5 min at 300x g followed by two washes in PBS. After incubation with 10 µg/mL RNase A for 5 min at RT, DNA was stained with 20 µg/mL propidium iodide and analysed using flow cytometry. Analysis of the data was performed using CellQuest Pro and ModFit LT software.

2.2.6 Immunoblotting

Cells were harvested by trypsinisation and resuspended in appropriate amounts of SDS-PAGE loading buffer (0.16 M Tris-HCl pH 6.8, 4% (v/v) SDS, 20% (v/v) glycerol, 0.01% (w/v) bromophenol blue, 100 mM DTT) to prepare whole-cell extracts. Samples were briefly sonicated, boiled at 70˚C for 10 min and centrifuged at 20,000 x g for 7 min. Relative protein concentrations were assessed using a spectrophotometer; equal amounts of protein were analysed by SDS-PAGE and immunoblotting.

Samples were loaded onto Bis-Tris or Tris-Acetate gels and separated at 180 V in MOPS or Tris-Acetate SDS running buffer (Invitrogen), respectively. Semi-dry transfer in transfer buffer (Invitrogen) with 10% (v/v) methanol was applied to transfer proteins onto a nitrocellulose membrane. To block non-specific binding sites, the membrane was incubated in blocking buffer (5% (w/v) dried skimmed milk in PBS-Tween (0.05% (v/v) Tween 20 in PBS)) for 1 h at RT. The protein of interest was detected by incubation with primary antibody (diluted in 2% (w/v) BSA and 0.05% (w/v) azide in PBS-Tween) overnight at 4˚C. The next day, the membrane was washed in PBS-Tween

three times for 5 min at RT. After incubation with secondary antibody diluted in blocking buffer for 1 h at RT, the membrane was washed in PBS-Tween three times for 10 min at RT. Subsequently, ECL western blotting detection reagent was used to detect proteins on X-ray films. A list of the antibodies and conditions used for immunoblotting can be found in Table 5 and Table 6.

2.2.7 Reverse-transcriptase quantitative PCR (RT-qPCR)

Cells were processed for RT-qPCR using the Power SYBR Green Cells-to-CT kit according to manufacturer's instructions. Reactions were performed in triplicate. All primers used for qPCR are summarised in Table 3. Primers against the housekeeping gene *B2M* were used as endogenous controls.

2.2.8 Immunofluorescence

Cells were washed in PBS and lysed in hypotonic solution (85.5 mM NaCl and 5 mM $MgCl_2$) for 5 min at RT. Next, cells were fixed with 4% (v/v) paraformaldehyde for 10 min at RT and permeabilised in 4% (v/v) paraformaldehyde supplemented with 0.03% (v/v) SDS. For immunofluorescence of RPA, cells were additionally fixed in 100% (v/v) ice-cold methanol for 5 min before permeabilisation. After washing in PBS with 0.4% (v/v) Photoflo and blocking with antibody dilution buffer (1% (v/v) goat serum, 0.3% (w/v) BSA, 0.005% (v/v) Triton X-100 in PBS), cells were incubated with primary antibody overnight at RT. On the next day, cells were washed three times in PBS with 0.4% (v/v) Photoflo and secondary antibody was added for 1 h. Following three washes as above, the coverslips were dried and mounted on microscope slides using the ProLong Antifade kit (Life Technologies) supplemented with 2 µg/mL DAPI. The

specimens were viewed with an inverted microscope and fluorescence imaging workstation equipped with an HCX Plan-Apochromat 100°- NA 1.4-0.7 oil objective. Images were acquired using a digital camera together with the LAS-AF software.

2.2.9 Telomeric FISH

Following overnight incubation with 0.1 µg/mL colcemid, mitotic cells were collected by mitotic shake-off and swollen in pre-warmed hypotonic buffer (0.03 M sodium acetate) at 37˚C for 25 min. Three drops of freshly prepared fixative (3:1 mix of methanol and acetic acid) were added to the cells followed by centrifugation at 650x g for 10 min. Then, the supernatant was aspirated leaving 1 mL for resuspending the cells. Eleven mL of fixative were added before the cells were pelleted by centrifugation again. After resuspending the pellet in 250 - 500 µL fixative, the cells were dropped onto slides pre-soaked in 45% (v/v) acetic acid and left to dry overnight. On the next day, the slides were washed in PBS for 15 min and fixed in 4% (v/v) formaldehyde (in PBS) for 2 min. The spread nuclei were digested in pepsin solution (0.1% (w/v) pepsin, 0.03% HCl (v/v)) at 37˚C for 10 min and fixed again in 4% (v/v) formaldehyde for 2 min. Afterwards, the slides were dehydrated by sequential washes in 70% (v/v), 90% (v/v) and 100% (v/v) ethanol. The dry slides were covered with the telomeric FISH probe mix and denatured at 80˚C for 3 min. After 2-h incubation at RT in the presence of a telomeric FISH probe, the slides were washed in formamide wash (70% (v/v) formamide, 10 mM Tris-HCl pH 7.5, 0.1% (w/v) BSA) twice for 15 min, followed by washes in PBS and dehydration as before. The air-dried slides were mounted in DAPI-containing Vectashield mix. Images were acquired using the same instrumentation as described for immunofluorescence.

2.2.10 Comet assay

The comet assay was performed as previously described (Parsons *et al.*, 2009). In brief, 2 x 10^5 cells were embedded in 1% (w/v) low-melting agarose in PBS on a microscope slide. Subsequently, the cells were lysed in buffer containing 2.5 M NaCl, 100 mM EDTA, 10 mM Tris-HCl pH 10.5, 1% (v/v) DMSO and 1% (v/v) Triton X-100 for 1 h at 4˚C. To denature the DNA, the slides were incubated in cold electrophoresis buffer (300 mM NaOH, 1 mM EDTA, 1% (v/v) DMSO, pH >13) for 30 min in the dark. Following electrophoresis at 25 V and 300 mA for 25 min, the DNA was neutralised with 0.5 M Tris-HCl pH 8.0. After staining with SYBR Gold, tail measurement was performed using the Komet 5.5 image analysis software.

2.2.11 DNA fibre assay

Cells were seeded in 6-well plates one day before labelling the DNA by addition of 4 µL of CldU solution (5 mg/mL stock) to 2.5 mL of media, followed by 30-min incubation at 37˚C. After three washes with warm PBS, 2 mL of fresh media containing 18 µL of IdU solution (10 mg/mL stock) were added to each well. Following incubation for 30 min at 37˚C, cells were harvested by trypsinisation and 2.5 x 10^6 cells were resuspended in cold PBS. Subsequently, labelled and unlabelled cells were combined at a 1:1 ratio. Next, 7.5 µL of lysis buffer (200 mM Tris-HCl pH 7.4, 50 mM EDTA, 0.5% (v/v) SDS) were mixed with 2.5 µL of cell suspension on a microscopy slide and incubated horizontally for 9 min at RT. The DNA was spread by tilting the slide manually at an angle of 30˚-45˚. The air-dried DNA was fixed in methanol/acetic acid (3:1) overnight at 4˚C. Slides were then rehydrated in PBS twice for 3 min and the DNA was denatured in 2.5 M HCl for 1 h at RT. The slides were washed several times in PBS until a pH of 7-7.5 was

reached, followed by incubation in blocking solution (2% (w/v) BSA, 0.1% (v/v) Tween 20, PBS; 0.22 µm filtered) for 40 min at RT and in primary antibodies (rat anti-CldU and mouse anti-IdU) for 2.5 h at RT. After five washes in PBS-Tween (0.2% (v/v) Tween 20 in PBS) for 3 min and one short wash in blocking solution, the slides were incubated with the secondary antibodies (anti-rat Cy3 and anti-mouse Alexa 488) for 1 h at RT. Subsequently, they were washed as before, air-dried and mounted in Antifade Gold. Images were acquired as described for immunofluorescence and analysed using ImageJ software.

2.2.12 Plasmid-based replication assay

The plasmid-based replication assay was performed as previously described (Follonier *et al.*, 2014), with modifications detailed below.

2.2.12.1 Plasmids

Dr. M. Lopes (University of Zurich) provided the original plasmid pML113 (Follonier *et al.*, 2014). Dr. P. Zawadzki, a previous lab member generated the variant plasmid pML113^{PURO}, which contains the puromycin resistance marker and enables selection of plasmid-containing cells. Into this plasmid we cloned two sequences with G4-forming potential (Table 4). Ten repeats of the telomeric sequence TTAGGG were integrated into pML113^{PURO} by blunt-end ligation into the PacI restriction site to generate the 10Telo-pML113^{PURO} plasmid. Oligonucleotides containing ten telomeric repeats were obtained from Sigma, annealed and ligated into pML113^{PURO} using the rapid DNA ligation kit. To generate the 1 Kb-telomere repeat vector, the sequence of interest was excised by restriction digest from a previously generated plasmid (pBluHCMV, a gift from Dr. E. Gilson, University of Nice; Table 4) and cloned into the PacI site of

pML113^{PURO}. The QIAquick PCR purification kit was used to purify DNA after restriction digest followed by agarose gel extraction of resulting restriction fragments using the QIAquick gel extraction kit. All constructs were transformed into competent *Escherichia coli* (*E. coli*) cells according to manufacturer's instructions (New England Biolabs*)*. Plasmid DNA was extracted from individual bacterial colonies using the QIAprep spin miniprep kit and restriction digest was performed to screen for positive clones. Selected plasmids were analysed by DNA sequencing and DNA from the correct clones was amplified and extracted using the QIAfilter plasmid maxi kit. All kits were used according to manufacturer's instructions.

2.2.12.2 Plasmid transfection and recovery

Five µg of plasmid DNA were transfected into RAD51-depleted and control HEK-293T cells using JetPRIME transfection reagent. After 40-h incubation at 37˚C, plasmid DNA was recovered according to the previously described protocol (Follonier *et al.*, 2014). HEK-293T cells were transfected with siRNA 80 h before plasmid recovery as described in section 2.2.2.

2.2.12.3 Replication efficiency determination

Approximately 1 µg of recovered DNA was mixed with 1x DNA loading buffer (6x DNA loading buffer: 0.25% (w/v) bromophenol blue, 0.25% (w/v) xylene cyanol FF, 10% (v/v) glycerol) and electrophoresed in a 0.7% agarose gel (0.7% (w/v) agarose in 1x TAE (50x TAE: 2 M Tris, 50 mM EDTA pH 8.0, 1 M acetic acid)). Replication efficiency was determined according to the intensity of bands and not to the Nanodrop reading because we observed that variable amounts of genomic DNA contaminated the plasmid preparation.

3 Results

3.1 Chemical ERK1/2 inhibition decreases viability of HR-deficient cells

ERK1/2 are components of the MAPK pathway upregulated in human tumours (Wagner *et al.*, 2009). Therefore, they represent attractive targets to exploit in the development of cancer therapeutics. To date, however, common problems with chemical ERK inhibitors have been cytotoxicity, poor cellular activity and insufficient selectivity. Recently, a novel ERK1/2 inhibitor, SCH772984, was identified, which exhibited high specificity and inhibitory potential in biochemical assays. Additionally, this compound was particularly potent in suppressing growth of tumours refractory to BRAF and MEK inhibitors (Morris *et al.*, 2013).

Previously, our lab reported that genetic inhibition of ERK1 expression with shRNA leads to a proliferative defect in BRCA2-deficient human and mouse cells (Carlos *et al.*, 2013). To test whether chemical ERK inhibition could trigger a similar effect, we performed dose-dependent viability assays in HR-proficient and -deficient human cells. In these cells, the expression of either RAD51 or BRCA2 was abrogated, both known to suppress recombinational DNA repair and to elicit similar cellular responses to DNA damage.

Treatment with the well-characterised ERK inhibitor VTX-11e (Aronov *et al.*, 2009) as well as the novel compound SCH772984 decreased the viability of BRCA2-depleted human HEK-293T cells in a dose-dependent manner (Figure 4a). The PARP inhibitor olaparib was used as a control for specific elimination of HR-deficient cells (McCabe *et al.*, 2006). Notably, olaparib and ERK inhibitor treatments only mildly obstructed proliferation of BRCA2-depleted cells (Figure 4a & b), probably due to insufficient

siRNA-mediated depletion of BRCA2 as determined by Western blotting (Figure 4c). Human BRCA2 is a high molecular weight protein (390 kDa) and inhibition of its expression using siRNA in HEK-293T cells has proven problematic, in spite of the established efficiency of this siRNA in other human cells lines (Carlos *et al.*, 2013). However, in similar assays (performed by E. Tacconi) V-C8 hamster cells with complete *BRCA2* deletion showed high sensitivity to all three drugs (Chaikuad *et al.*, 2014).

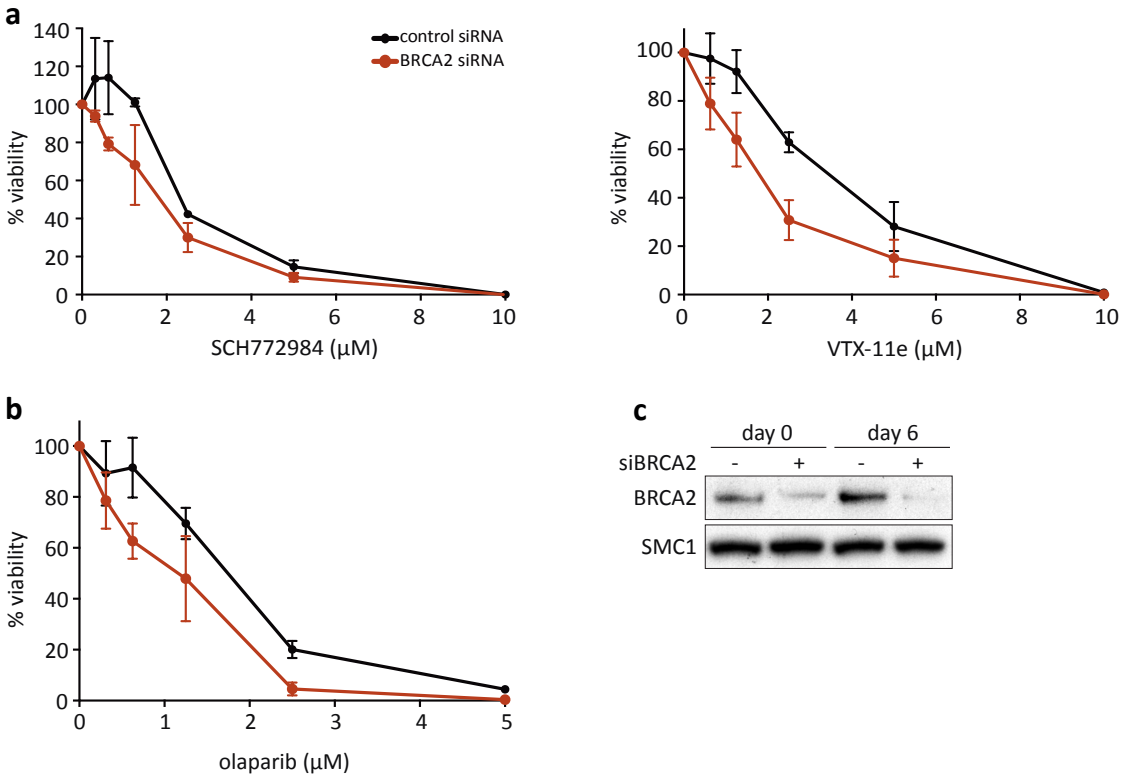

Figure 4: ERK1/2 inhibition reduces proliferation of BRCA2-deficient cells
Human HEK-293T cells were transfected with control or BRCA2 siRNA three times at three-day intervals. One day after the first transfection, chemical compounds were added to the media at the indicated concentrations and treatment was continued for six days. Graphs are representative of two independent experiments, each performed in triplicate. Error bars represent s.d. of triplicate values obtained from a single experiment. (**a**) Dose-dependent viability assays performed in cells treated with ERK inhibitors SCH772984 or VTX-11e. (**b**) Dose-dependent viability assays performed in cells treated with the PARP inhibitor olaparib. (**c**) Whole-cell extracts prepared at the time when inhibitor treatment was initiated (day 0) and terminated (day 6) were immunoblotted as indicated. SMC1 was used as a loading control.

To examine the validity of these results in cells lacking another HR activity, we next inhibited expression of the key HR protein RAD51 using siRNA.

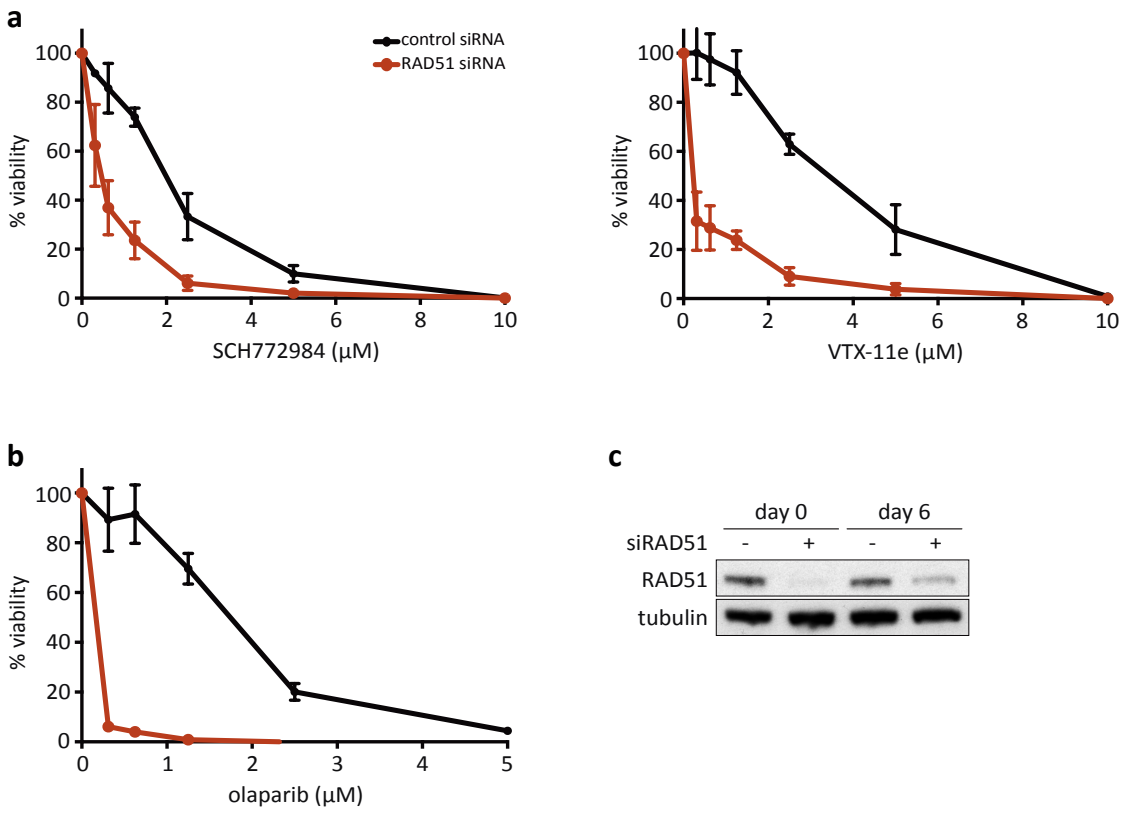

Figure 5: ERK1/2 inhibition reduces proliferation of RAD51-deficient cells
Human HEK-293T cells were transfected with control or RAD51 siRNA three times at three-day intervals. One day after the first transfection, chemical compounds were added to the media at the indicated concentrations and treatment was continued for six days. Graphs are representative of two independent experiments, each performed in triplicate. Error bars represent s.d. of triplicate values obtained from a single experiment. (**a**) Dose-dependent viability assays performed in cells treated with ERK inhibitors SCH772984 or VTX-11e. (**b**) Dose-dependent viability assays performed in cells treated with the PARP inhibitor olaparib. (**c**) Whole-cell extracts prepared at the time when inhibitor treatment was initiated (day 0) and terminated (day 6) were immunoblotted as indicated. Tubulin was used as a loading control.

Both ERK inhibitors, SCH772984 and VTX-11e, triggered a specific, dose-dependent growth arrest in siRAD51-treated cells (Figure 5a). The PARP inhibitor olaparib also had a significant anti-proliferative effect in RAD51-depleted cells (Figure 5b).

Immunoblotting of whole-cell extracts confirmed efficient depletion of RAD51 during the six-day inhibitor treatment (Figure 5c).

Overall, our results are consistent with previous genetic studies and support the concept that chemical ERK inhibition allows for selective targeting of HR-deficient cells.

3.2 G4 stabilisation results in reduced viability of HR-deficient cells

Stable G4s are deleterious to cell viability, as they block replication fork progression and cause DNA breakage. In HR-deficient cells, stalled replication forks represent a source of genomic instability, and we reasoned that the additional replication burden imposed by persistent G4s would be particularly toxic. To investigate the effect of G4 stabilisation in HR-deficient mammalian cells as a potential strategy for eliminating HR-deficient cells, we used two compounds with high G4 binding affinity. $PhenDC_3$ and pyridostatin are both known to stabilise G4s by enhancing their thermal stability. Additionally, both compounds have been shown to display a high selectivity for G4s versus duplex DNA (De Cian *et al.*, 2007; Monchaud *et al.*, 2008; Müller *et al.*, 2010; Rodriguez *et al.*, 2008). Notably, $PhenDC_3$ and pyridostatin are universal G4 ligands that bind polymorphic G4 structures with variable DNA sequences (De Cian *et al.*, 2007; Gomez *et al.*, 2010; Halder *et al.*, 2011; Halder *et al.*, 2012; Lopes *et al.*, 2011; Monchaud *et al.*, 2008; Müller *et al.*, 2010; Piazza *et al.*, 2010; Rodriguez *et al.*, 2008), which makes them suitable for genome-wide assays.

Firstly, we performed resazurin-based viability assays to determine whether G4 stabilisation could specifically decrease the proliferative capacity of HR-deficient cells. In these assays, we used the well-characterised BRCA2-deficient hamster cell line V-C8

(Kraakman-van der Zwet *et al.*, 2002) and the control cell line complemented with full-length *BRCA2* cDNA as a control.

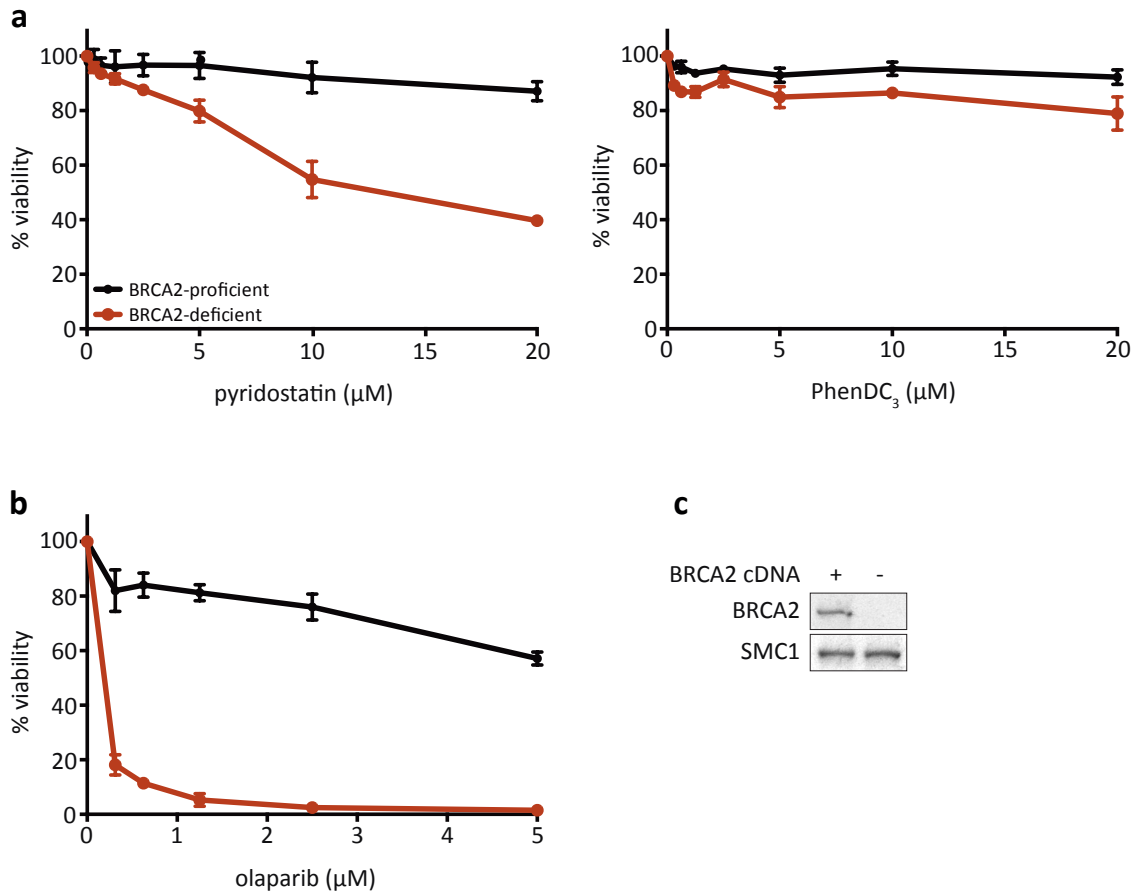

Figure 6: G4 stabilisation specifically inhibits proliferation of BRCA2-deficient hamster cells
BRCA2-proficient and -deficient V-C8 cells were treated with the indicated concentrations of chemical inhibitors for three or six days. Graphs are representative of two independent experiments, each performed in triplicate. Error bars represent s.d. of triplicate values obtained from a single experiment. (**a**) Dose-dependent viability assays performed in cells treated with G4 stabilising compounds pyridostatin or $PhenDC_3$ for six days as described above. (**b**) Dose-dependent viability assays performed in cells treated with the PARP inhibitor olaparib for three days as described above. (**c**) Whole-cell extracts prepared from BRCA2-positive and -negative V-C8 cell lines were immunoblotted as indicated. SMC1 was used as a loading control.

Both G4 stabilisers, pyridostatin and $PhenDC_3$, significantly decreased the proliferative capacity of V-C8 hamster cells lacking BRCA2 compared to control BRCA2-complemented cells in a dose-dependent manner (Figure 6a). V-C8 cells were also hypersensitive to olaparib (Figure 6b), as previously reported (Bryant *et al.*, 2005).

Immunoblotting confirmed that the V-C8 cell line lacked BRCA2 expression, whereas the complemented one expressed full-length BRCA2 (Figure 6c).

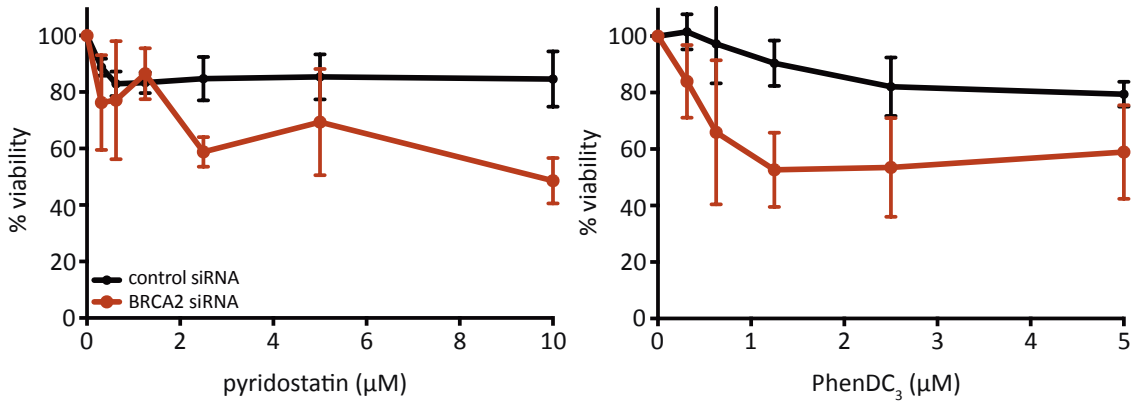

Figure 7: G4 stabilisation specifically inhibits proliferation of BRCA2-deficient human cells
Human HEK-293T cells were transfected with control or BRCA2 siRNA three times at three-day intervals. One day after the first transfection, pyridostatin or $PhenDC_3$ was added to the media at the indicated concentrations and treatment was continued for six days. Dose-dependent viability graphs are representative of two independent experiments, each performed in triplicate. Error bars represent s.d. of triplicate values obtained from a single experiment.

Secondly, we addressed whether G4 stabilisers have an anti-proliferative effect in human cells lacking HR activities. Thus, cell viability was determined in human HEK-293T cells treated with increasing concentrations of pyridostatin or $PhenDC_3$, in which BRCA2 (Figure 7) or RAD51 (Figure 8) knockdown was induced using siRNA. Cells treated with AllStar siRNA were used as a control in these experiments. G4 stabilisation by either pyridostatin or $PhenDC_3$ induced a marked reduction in proliferation of cells lacking BRCA2 (Figure 7) or RAD51 (Figure 8). These results indicated that persistent G4s are deleterious in the context of HR deficiency in human cells.

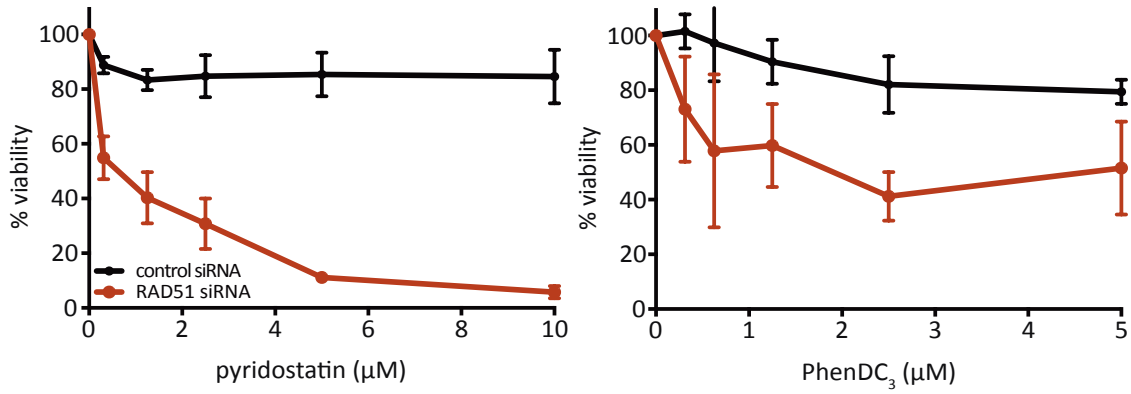

Figure 8: G4 stabilisation specifically inhibits proliferation of RAD51-deficient human cells
Human HEK-293T cells were transfected with control or RAD51 siRNA three times at three-day intervals. One day after the first transfection, pyridostatin or $PhenDC_3$ was added to the media at the indicated concentrations and treatment was continued for six days. Dose-dependent viability graphs are representative of two independent experiments, each performed in triplicate. Error bars represent s.d. of triplicate values obtained from a single experiment.

To address whether G4 stabilisation leads solely to a proliferative arrest or also to cell death, we examined expression of cleaved PARP, a well-established apoptosis marker (Oliver *et al.*, 1998), using immunoblotting of HR-deficient cells exposed to pyridostatin or $PhenDC_3$ (Figure 9). In the same assay, we evaluated accumulation of DNA damage since G4 stabilisation is known to cause replication fork stalling and generate DNA breaks (Rodriguez *et al.*, 2012). This analysis revealed that the expression levels of cleaved PARP were significantly increased after treatment with $PhenDC_3$ or pyridostatin specifically in HR-deficient cells (Figure 9) suggesting that HR is essential for cell survival in the presence of G4-interacting drugs. RAD51 inhibition by itself also induced detectable levels of apoptosis (Figure 9). Furthermore, in drug-treated cells lacking RAD51 we observed elevated phosphorylation of the histone protein variant H2AX on Ser139 (γH2AX), a well-established DNA damage marker (Rogakou *et al.*, 1999), compared to control cells (Figure 9). Collectively, these data indicate that G4 stabilisation triggers specific killing of HR-deficient cells through accumulation of DNA damage.

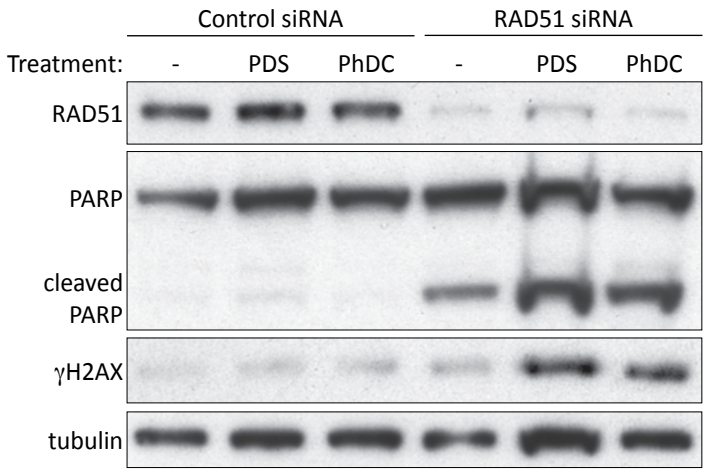

Figure 9: G4 stabilisation induces apoptosis and DNA damage in HR-deficient cells
Human HEK-293T cells were transfected with control or RAD51 siRNA twice at an interval of three days. One day after the first transfection, pyridostatin or $PhenDC_3$ (2 μM) was added to the media. Whole-cell extracts prepared after four days of treatment were immunoblotted as indicated. Tubulin was used as a loading control. PDS, pyridostatin; PhDC, $PhenDC_3$.

3.3 Pyridostatin induces DNA damage

Viability assays performed in RAD51-deficient HEK-293T cells demonstrated that pyridostatin exhibited a more potent anti-proliferative effect than $PhenDC_3$ (Figure 8). Thus, we concentrated on this compound and investigated in detail the cellular responses to this drug in the context of HR deficiency mediated by RAD51 knock down. In particular, we studied the DNA damage response induced by pyridostatin treatment, given the increase in the levels of γH2AX detected after exposure to this drug (Figure 9).

Firstly, the amount of DNA breaks after four days of treatment was estimated using comet assays. In these assays, the percentage of tail DNA relative to total DNA was indicative of the levels of DNA damage present in an individual cell. Pyridostatin caused an increase in DNA damage, which was significantly higher in HR-deficient cells treated with pyridostatin compared to untreated cells (Figure 10).

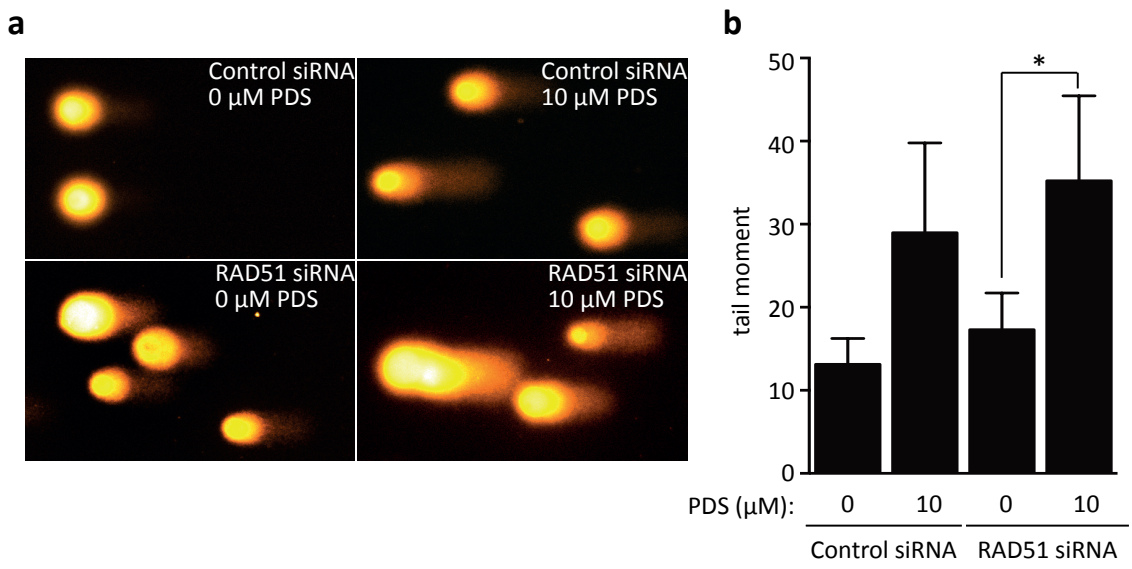

Figure 10: Pyridostatin induces DNA damage detected with comet assays
Human HEK-293T cells were transfected with control or RAD51 siRNA twice at an interval of three days. One day after the first transfection, pyridostatin (10 µM) was added to the media and comet assays were performed after four days of treatment. (**a**) Representative images of nuclei from cells exposed to indicated treatments. (**b**) Quantification of tail moment in cells treated as above (n=4; error bars, s.d.). *P* values were calculated using an unpaired two-tailed *t*-test with Welch's correction (*, $P \leq 0.05$). PDS, pyridostatin.

Secondly, formation of γH2AX foci was determined using immunofluorescence staining of fixed cells with an anti-γH2AX antibody (Figure 11). Quantification of three independent experiments revealed a significant increase in the frequency of HR-deficient cells containing five or more γH2AX foci after pyridostatin treatment (Figure 11b). On average, 16.5% of untreated siRAD51-depleted cells exhibited five or more foci, which escalated to 37.3% and 55.4% following treatment with 2 µM and 10 µM pyridostatin, respectively (Figure 11b). The percentage of control cells with five or more foci rose from 4.5% to 8.2% and 9.7% after exposure to the indicated concentrations of pyridostatin, an increase that was not statistically significant (Figure 11b).

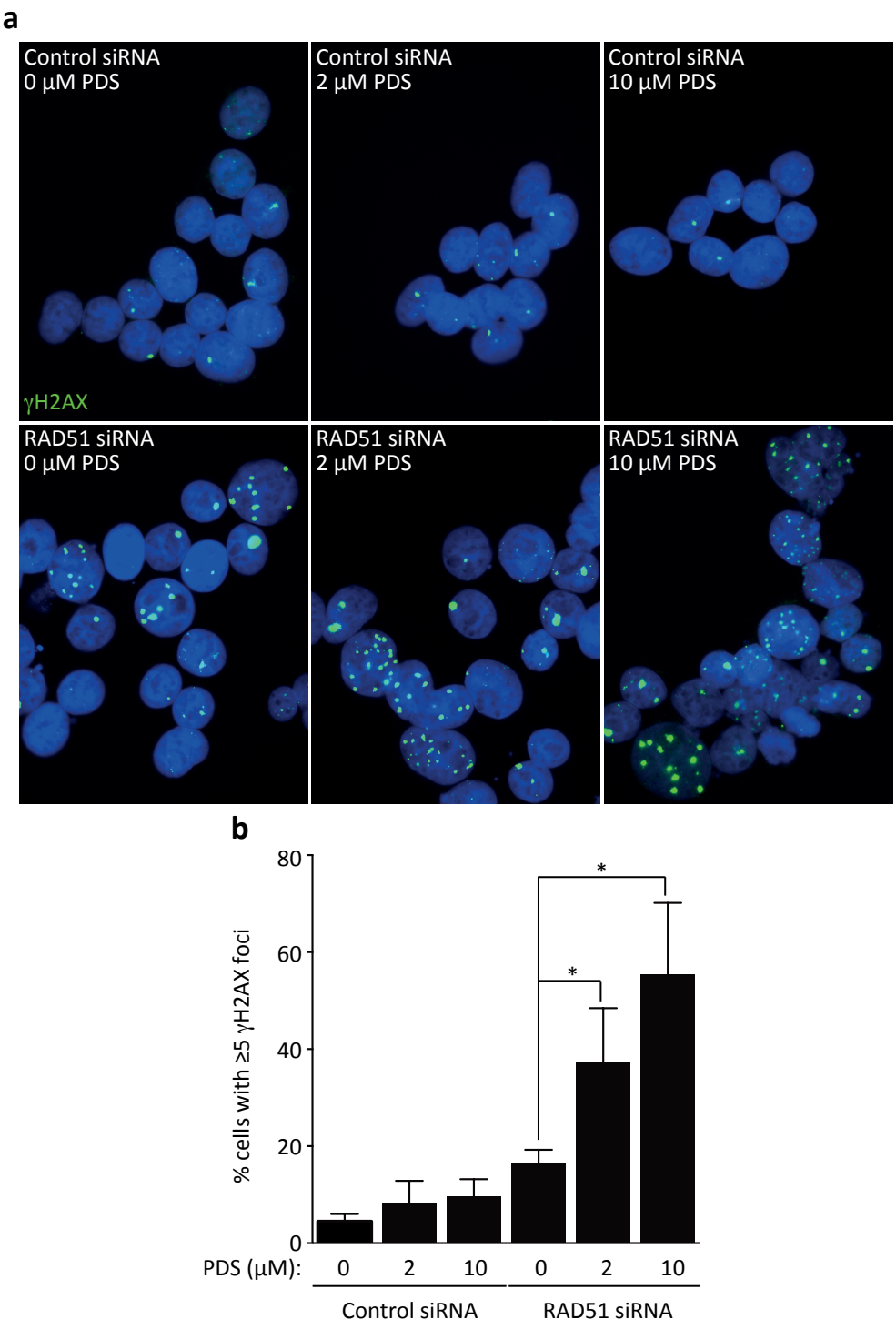

Figure 11: Pyridostatin triggers γH2AX foci formation

Human HEK-293T cells were transfected with control or RAD51 siRNA twice at an interval of three days. One day after the first transfection, pyridostatin was added to the media at the indicated concentrations. Cells were processed for immunofluorescence staining after four days of treatment. (**a**) Representative images of γH2AX foci after indicated treatment. (**b**) Quantification of the frequency of cells with ≥5 γH2AX foci in cells treated as above (n=3; error bars, s.d.). *P* values were calculated using an unpaired two-tailed *t*-test (*, $P \leq 0.05$ and **, $P \leq 0.01$). PDS, pyridostatin.

Thirdly, the frequency of chromatid and chromosome breaks was directly assessed as a measure of DSB accumulation using mitotic chromosome spreads (Figure 12). We observed significantly elevated numbers of DSBs per metaphase following pyridostatin treatment, whilst RAD51 depletion further enhanced this effect (Figure 12b). Noteworthy, non-depleted cells treated with 10 µM pyridostatin exhibited very similar numbers of DSBs per metaphase as untreated RAD51-depleted cells (Figure 12b). Since both, pyridostatin-treated control and untreated RAD51-depleted HEK-293T cells, are largely viable, this suggests that cells exceeding five chromosome/chromatid breaks are likely to encounter mitotic catastrophe and be eliminated.

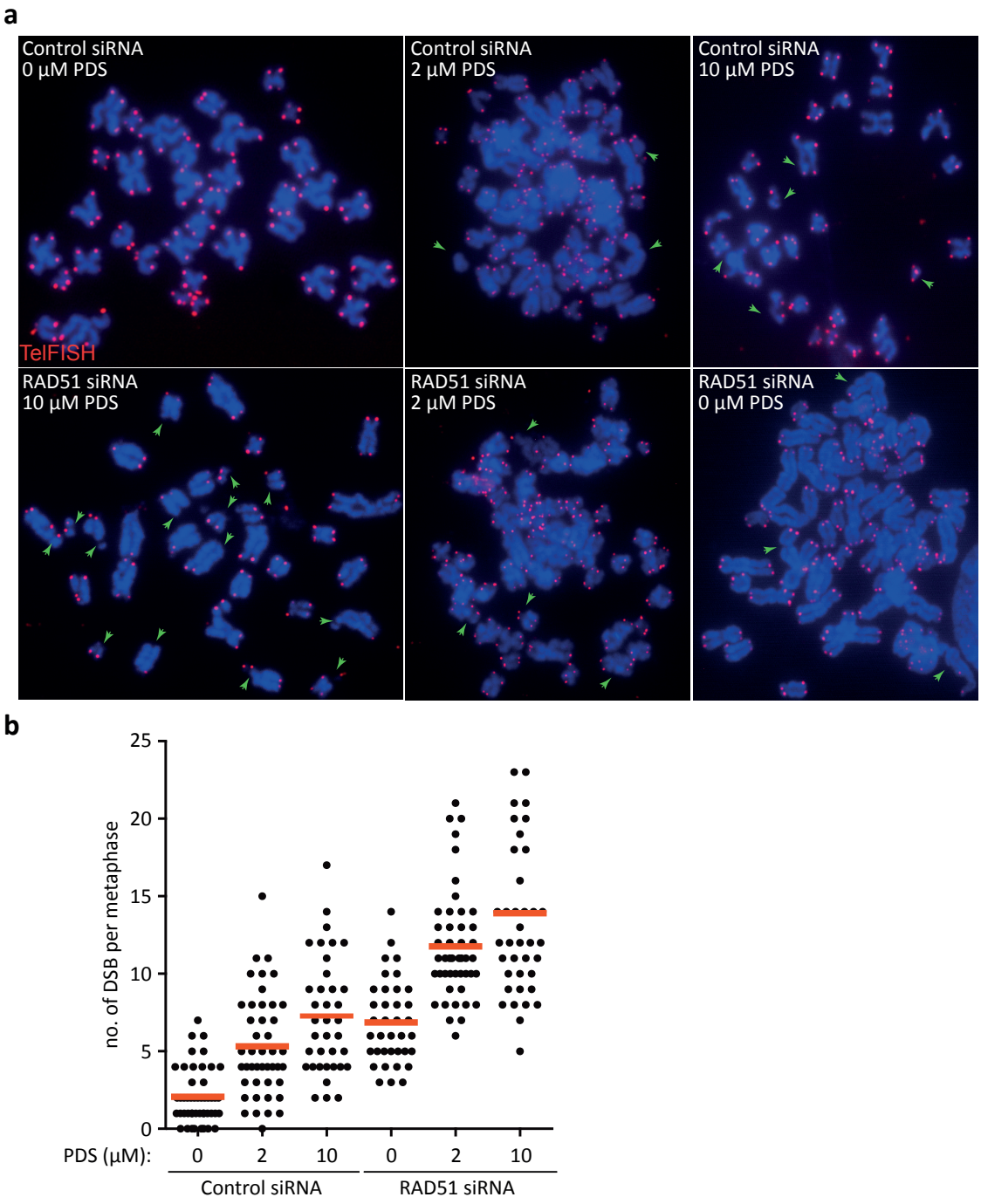

Figure 12: Pyridostatin induces DNA DSBs visualised on mitotic chromosomes
Human HEK-293T cells were transfected with control or RAD51 siRNA twice at an interval of three days. One day after the first transfection, pyridostatin was added to the media at the indicated concentrations for four days. (**a**) Cells treated as above were incubated overnight with colcemid and processed for FISH analysis of metaphase chromosome spreads with a Cy3-conjugated telomeric probe (red). Arrowheads point to chromatid/chromosome breaks. (**b**) Quantification of chromatid/chromosome break frequencies in cells treated as in (**a**). A minimum of 35 metaphases were analysed for each sample. Red bars indicate mean frequencies of breaks. PDS, pyridostatin.

Taken together, these results are consistent with the notion that G4 stabilisation by pyridostatin induces DNA damage, which is more pronounced and has lethal consequences in HR-defective cells.

3.4 Pyridostatin triggers checkpoint activation and replication stress

We have shown that G4 stabilisation triggers DNA damage, reduced proliferation and apoptosis, all of which are enhanced in HR-compromised cells (Figure 6 - Figure 12). Thus, we addressed next whether ATM and/or ATR-dependent DDRs are activated and whether this leads to a proliferative arrest at a particular stage of the cell cycle.

ATM is a kinase that is activated in response to DSBs (Shiloh, 2006) and in turn phosphorylates the checkpoint kinase CHK2 (Brown *et al.*, 1999; Chaturvedi *et al.*, 1999; Matsuoka *et al.*, 1998). We detected phosphorylation of both, ATM and CHK2, in HR-deficient cells treated with pyridostatin (Figure 13) supporting the concept that the DSB accumulation observed after treatment with G4-stabilising compounds triggered an ATM-dependent checkpoint response.

Additionally, CHK1 was also phosphorylated upon pyridostatin treatment in cells lacking RAD51 (Figure 13). CHK1 is a well-established ATR target (Liu *et al.*, 2000; Lopez-Girona *et al.*, 2001; Walworth *et al.*, 1996). In contrast to ATM, ATR is responsible for sensing various types of DNA damage including DSBs, crosslinks, base adducts, and replication stress in general. Most studies, however, suggest that ssDNA is primarily required for ATR activation (Costanzo *et al.*, 2003; Zou *et al.*, 2003). To protect DNA overhangs from degradation, cellular ssDNA, including that generated during DNA replication and repair, is coated by RPA (Fanning *et al.*, 2006). Accordingly, we detected an increase in RPA expression levels following G4 stabilisation especially

in HR-deficient cells (Figure 13), indicative of ssDNA accumulation. Moreover, RPA phosphorylation occurred in the same cells reflecting checkpoint activation (Figure 13). Collectively, these data demonstrate that both ATM- and ATR-dependent checkpoints are activated by pyridostatin in RAD51-depleted cells.

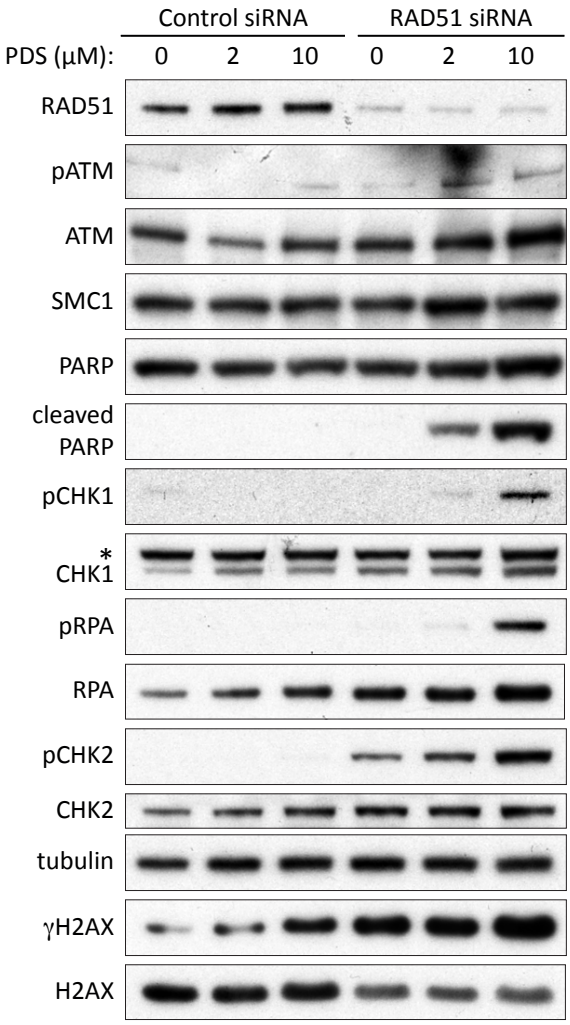

Figure 13: Pyridostatin causes DNA damage, checkpoint activation and apoptosis in HR-deficient cells

Human HEK-293T cells were transfected with control or RAD51 siRNA twice at an interval of three days. One day after the first transfection, pyridostatin was added to the media at the indicated concentrations. Whole-cell extracts prepared after four days of treatment were immunoblotted as indicated. Tubulin and SMC1 were used as loading controls. PDS, pyridostatin. *, non-specific band.

CHK1 and CHK2 phosphorylation are known to mediate G2/M arrest (Liu *et al.*, 2000). Therefore, we next performed FACS analyses (Figure 14) to determine whether pyridostatin caused a block in cell proliferation at a specific stage of the cell cycle. Untreated HR-proficient and -deficient cells showed a very similar cell cycle distribution profile with a mean of 20% of cells in the G2/M phase of the cell cycle (Figure 14b). After two days of treatment with 10 µM pyridostatin, the percentage of control cells in G2/M phase increased to a mean of about 30%, whereas almost 50% of HR-deficient cells accumulated in G2/M (Figure 14b). These results indicated that DSB accumulation upon pyridostatin treatment leads to checkpoint activation, which arrests cell cycle progression specifically in G2/M phase.

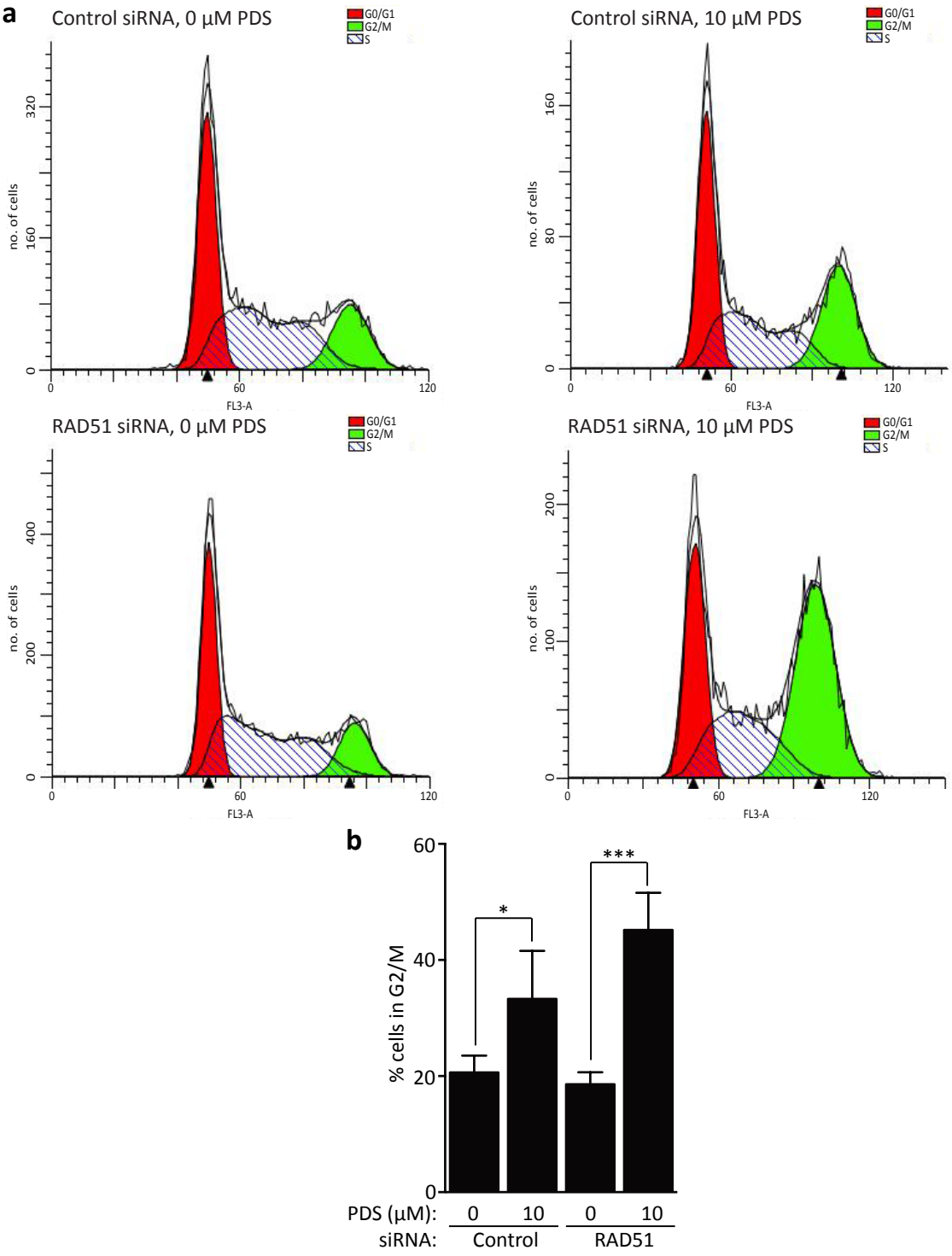

Figure 14: Pyridostatin leads to G2/M cell cycle arrest

One day after transfection of human HEK-293T cells with control or RAD51 siRNA, pyridostatin (10 µM) was added to the media and FACS analyses of DNA content were performed after two days of treatment. (**a**) Cell cycle distribution of cells exposed to the indicated treatments. Graphs are representative of four independent experiments. (**b**) Quantification of the percentage of cells in G2/M treated as above (n=4, error bars, s.d.). *P* values were calculated using an unpaired two-tailed *t*-test (*,$P \leq 0.05$ and ***, $P \leq 0.001$). PDS, pyridostatin.

Elevated RPA levels reflect ssDNA accumulation, indicative of replication stress (Zeman *et al.*, 2014). To determine whether under our experimental conditions RPA was bound to the chromatin and therefore identified sites of ssDNA, we visualised RPA foci by immunofluorescence and quantified their frequency (Figure 15).

A significant increase (8.75-fold) in cells exhibiting ten or more foci per cell was observed in HR-proficient cells and a higher increase (12.12-fold) in HR-deficient cells after treatment with pyridostatin compared to untreated cells (Figure 15b). This demonstrates that ssDNA levels are enhanced by pyridostatin treatment, and the effect is more pronounced in cells lacking HR activity.

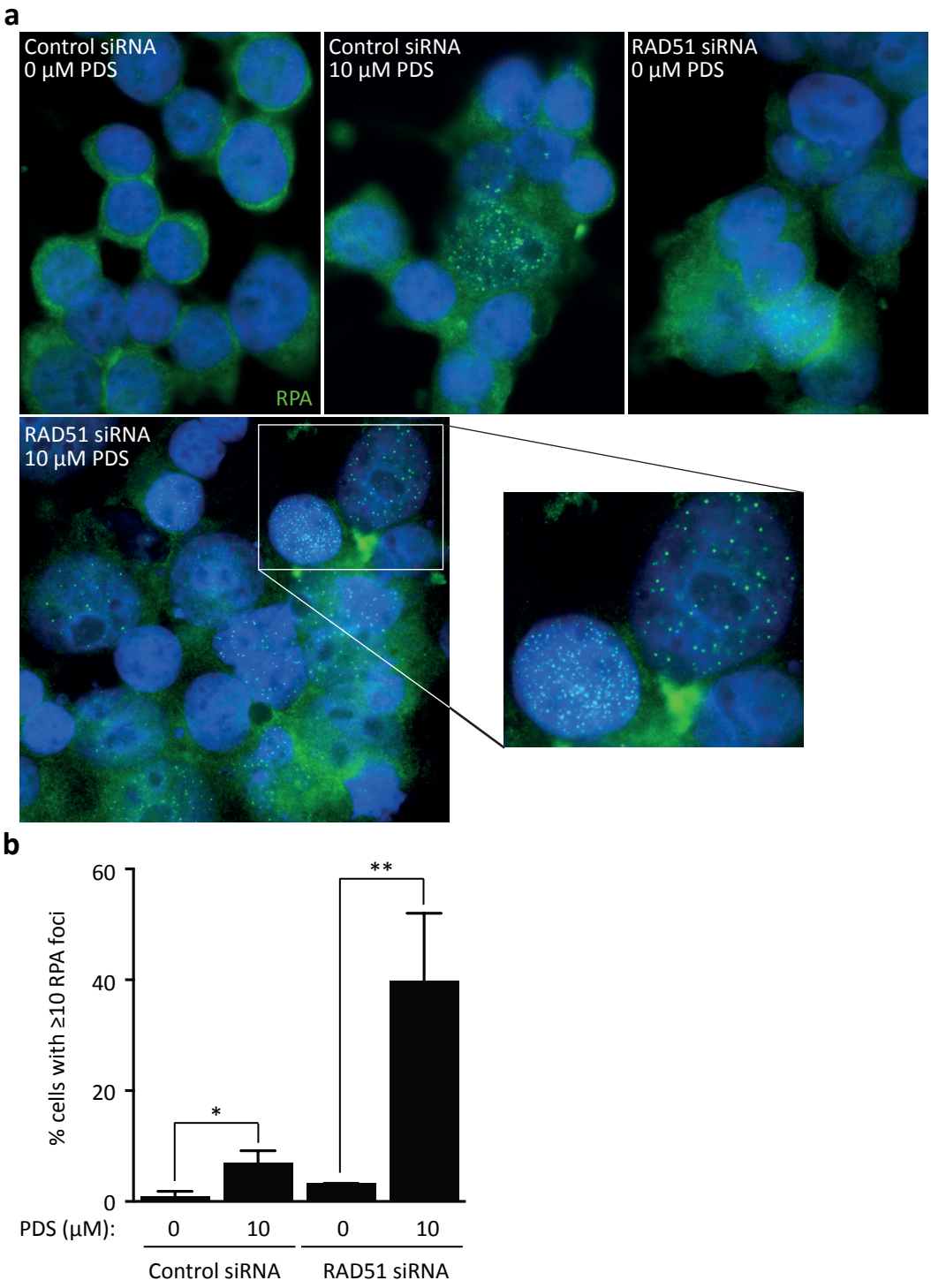

Figure 15: Pyridostatin triggers RPA foci formation

Human HEK-293T cells were transfected with control or RAD51 siRNA twice at an interval of three days. One day after the first transfection, pyridostatin (10 µM) was added to the media and cells were processed for immunofluorescence staining after four days of treatment. (**a**) Representative images of RPA foci after indicated treatment. (**b**) Quantification of the frequency of cells with ≥10 RPA foci in cells treated as above (n=3; error bars, s.d.). *P* values were calculated using an unpaired two-tailed *t*-test (*, $P \leq 0.05$ and **, $P \leq 0.01$). PDS, pyridostatin.

CHK1 activation and accumulation of RPA foci are strong indications of replication stress (Marechal *et al.*, 2013; Nam *et al.*, 2011). Therefore, we performed DNA fibre analyses to directly measure the rate of DNA synthesis and potentially obtain direct evidence for replication stress triggered by G4 stabilisation (Figure 16). In cells treated with control siRNA, pyridostatin triggered a significant reduction in replication tract length (from 17 µm to 9 µm) (Figure 16b). In addition, the tract length of untreated cells lacking RAD51 (10 µm) was shorter than of control cells (17 µm) (Figure 16b), as previously reported (Petermann *et al.*, 2010). Importantly, treatment with pyridostatin resulted in replication tracts with an average length of 9 µm in control siRNA-treated cells, whilst in RAD51 siRNA-treated cells tract length was further reduced to 2.5 µm after pyridostatin treatment. This difference was also statistically significant ($P < 0.0001$) (Figure 16b). These results indicate that G4 stabilisation has an additive effect on HR abrogation in obstructing replication fork progression, which could explain the observed toxicity of G4-binding compounds to HR-deficient cells.

Additionally, pyridostatin led to increased origin firing and replication fork stalling in both, HR-proficient and -deficient cells (Figure 16c & d). These observations further support the concept that G4 stabilisation potentiates the replication stress triggered by HR abrogation (Ge *et al.*, 2010; Ibarra *et al.*, 2008; Woodward *et al.*, 2006; Zeman *et al.*, 2014).

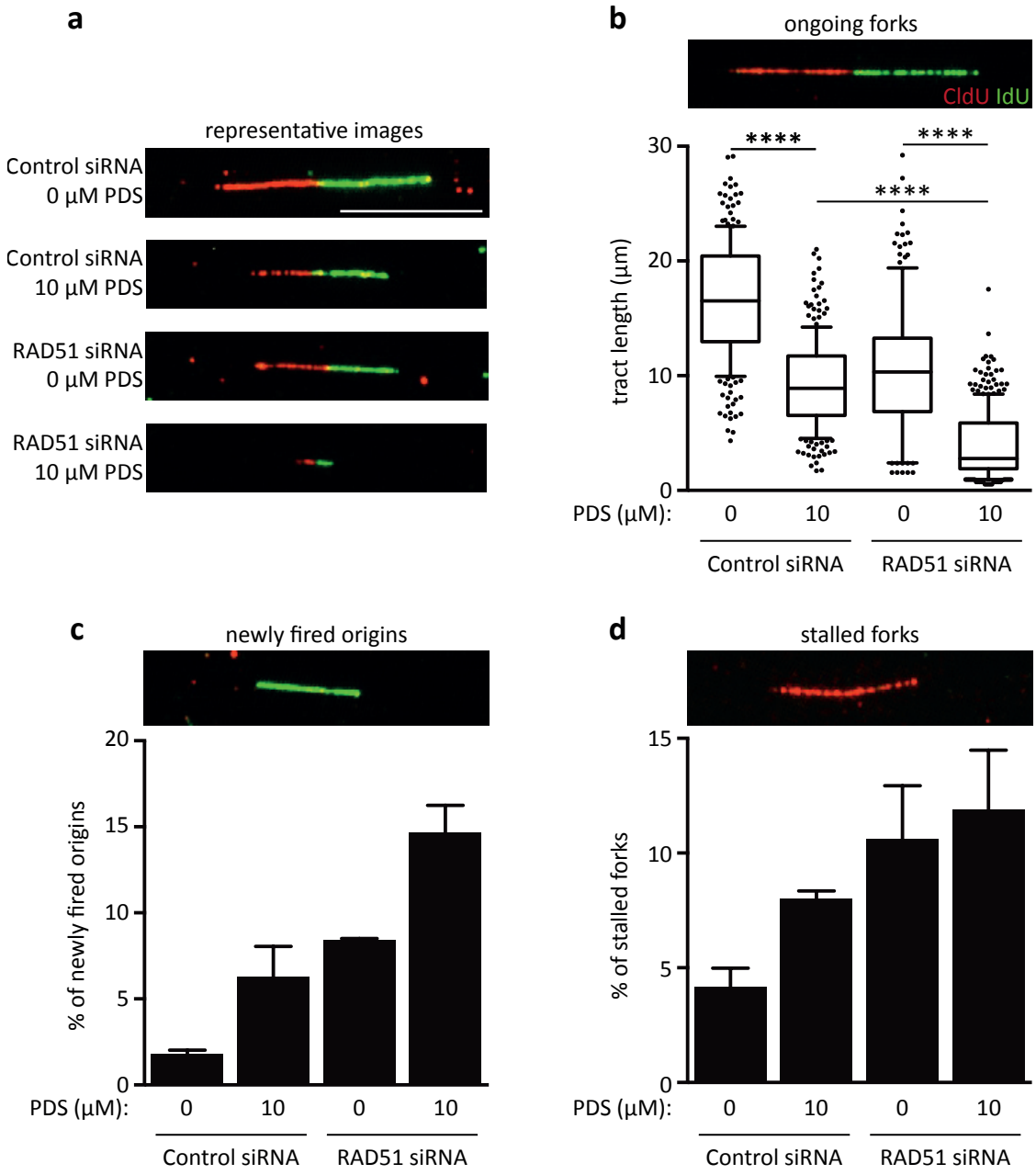

Figure 16: Pyridostatin induces replication stress

One day after transfection of human HEK-293T cells with control or RAD51 siRNA, pyridostatin (10 µM) was added to the media and cells were processed for DNA fibre analysis after two days of treatment. (**a**) Representative images of DNA fibres induced by the indicated treatments. Scale bar, 10 µm. (**b**) Quantification of the tract length in cells treated as above (n=2, error bars, s.d.). *P* values were calculated using an unpaired two-tailed *t*-test (****, $P \leq 0.0001$). (**c**) and (**d**) Quantification of the frequency of newly fired origins and stalled forks in cells treated as above. PDS, pyridostatin.

3.5 Pyridostatin decreases transcription of G4-containing genes

Thus far, we have demonstrated that G4 stabilisation causes DNA damage and replication stress, both enhanced in the context of HR deficiency. Next, we asked whether pyridostatin treatment, known to affect the transcription levels of genes containing sequences with high G4-forming potential in various cell lines (Kikin *et al.*, 2006; Rodriguez *et al.*, 2012), has a similar effect in the context of HR deficiency. We therefore measured mRNA levels of genes whose expression had previously been reported to be altered by pyridostatin treatment (*MYC*, *SRC* and *SREBF1*) (Rodriguez *et al.*, 2012) using RT-qPCR. *ALAS1* mRNA was used as a negative control due to the predicted low G4-forming potential of the DNA sequence of this gene (Kikin *et al.*, 2006).

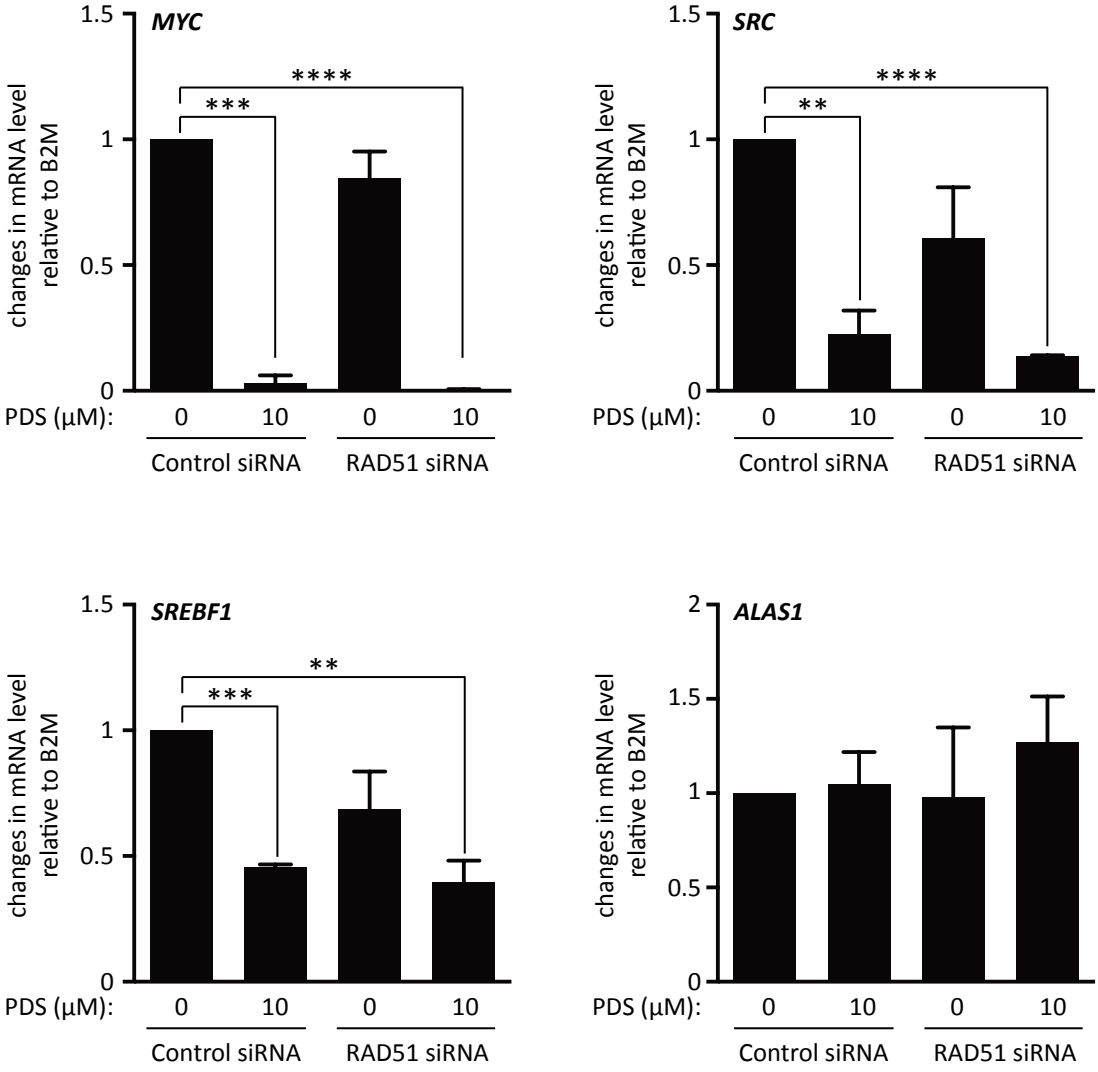

Figure 17: mRNA levels of G4-containing genes are downregulated by pyridostatin
One day after human HEK-293T cells were transfected with control or RAD51 siRNA, pyridostatin (10 μM) was added to the media. Expression levels of the indicated genes were determined using RT-qPCR after two days of treatment. mRNA levels were first normalised to the housekeeping gene *B2M* and then to the untreated samples (n=2, error bars, s.d.). *P* values were calculated using an unpaired two-tailed *t*-test (**, $P \leq 0.01$, ***, $P \leq 0.001$, ****, $P \leq 0.0001$). PDS, pyridostatin.

We observed that, within two days after the initiation of the treatment, the mRNA levels of the G4-containing genes were significantly reduced relative to untreated cells both in the presence and absence of RAD51 (Figure 17). Transcription of *ALAS1* was not affected either by pyridostatin or RAD51 siRNA treatment.

3.6 Evaluating replication efficiency of G4 sequences using a SV40-based plasmid replication assay

Replication origins in human genomic DNA are poorly defined, although recent studies using ChIP-seq approaches have helped mapping some of them (Mechali, 2010; Mechali *et al.*, 2013), and in general replication studies at specific genomic loci *in vivo* have been difficult to implement in human cells. To overcome this problem, Simian Virus 40 (SV40) has been used as a model for DNA replication in mammalian cells (Fanning *et al.*, 2009). The rationale for employing this system is that the small circular genome of SV40 is replicated by the same set of cellular proteins as mammalian genomic DNA. The only additional factor needed for SV40 replication is the viral helicase large T antigen (Tag), which provides the advantage that the SV40 genome is replicated several times in every cell cycle (Sogo *et al.*, 1986). Hence, SV40-based plasmids allow for efficient DNA amplification upon transfection into human cells. Recently, Follonier *et al.* reported an experimental system based on a SV40-derived plasmid, which allows to study the replication efficiency of repetitive DNA sequences *in vivo* (Follonier *et al.*, 2014) and to determine the genetic requirements for replicating such sequences. This system is superior to other previously developed plasmid replication assays because it enables recovery of large amounts of replication intermediates, which can be quantified and visualised by electron microscopy.

We used this plasmid-based replication assay to determine whether the replication efficiency of plasmids containing G4-forming sequences was altered in RAD51-depleted HEK-293T cells compared to non-depleted cells. Telomeric sequences are among the best-characterised DNA sequences with G4-forming potential (Parkinson *et al.*, 2002). We therefore cloned DNA fragments consisting of 60 bp or 1

Kb of TTAGGG telomeric repeats into the pML113^{PURO} plasmid in the proximity of the SV40 replication origin. These constructs and the control plasmid without insert were transfected into HEK-293T cells, which were previously treated with control or RAD51 siRNAs. Depletion of RAD51 was determined by immunoblotting (Figure 18a).

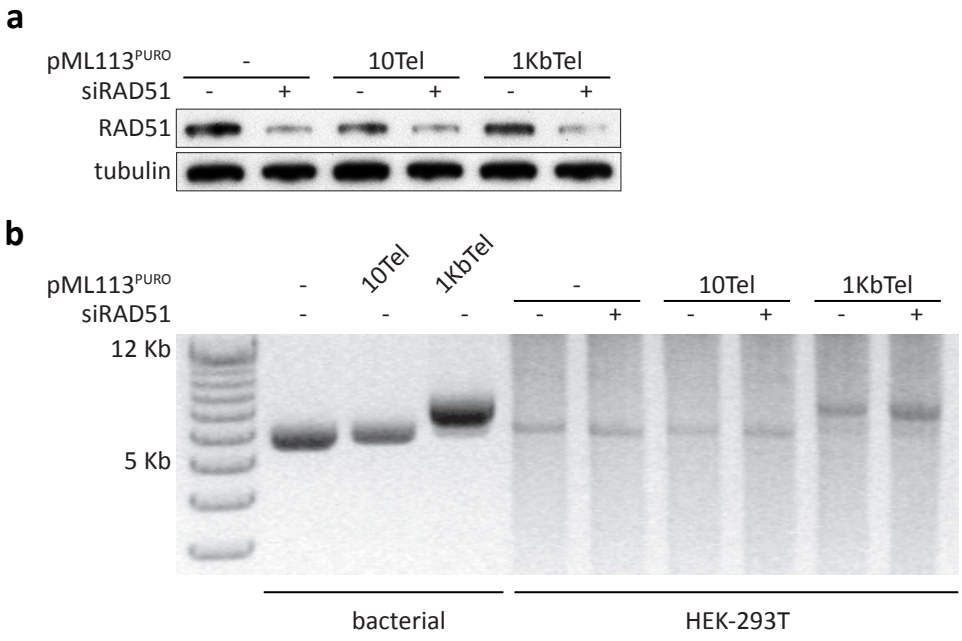

Figure 18: Recovery of plasmids containing sequences with G4-forming potential from HR-proficient and -deficient cells
(**a**) Human HEK-293T cells were transfected with control or RAD51 siRNA, one day before transfection with 5 µM plasmid DNA. Whole-cell extracts prepared 40 h after the second transfection were immunoblotted as indicated. Tubulin was used as a loading control. (**b**) Plasmid DNA extracted from cells treated as in (**a**) was linearised and separated using 0.7% agarose gel electrophoresis. Plasmid DNA extracted from bacteria was used as a control.

The plasmids were allowed to replicate for 40 h before plasmid DNA was extracted and quantified by gel electrophoresis. No difference was detected between the amount of plasmid DNA recovered from HR-proficient and -deficient cells. This observation was true for the control plasmid pML113^{PURO} as well as its derivatives 10Tel-pML113^{PURO} and 1KbTel-pML113^{PURO} that had G4-forming potential (Figure 18b). A possible explanation for these results is that G4-forming regions may not constitute

replication barriers when cloned into the SV40-derived plasmid, possibly due to the high processivity of the Tag viral helicase. Alternatively, SV40-driven DNA replication may in some aspects be mechanistically distinct from conventional cellular replication and may not require HR for bypassing potential obstructions.

4 Discussion

4.1 Chemical ERK inhibition selectively affects proliferation of HR-compromised cells

We have recently shown that shRNA-mediated depletion of ERK1, but not ERK2, selectively targets and kills HR-deficient cells. Moreover, this study reported a similar effect of chemical MEK1/2 inhibition on the viability of these cells (Carlos *et al.*, 2013). MEK1/2 are kinases of the MAPK pathway, which act upstream of ERK1/2 and activate them through phosphorylation. Several commercially available ERK1/2 inhibitors were also tested at the time in similar assays, however they showed high cellular toxicity irrespective of the cells' HR status (A. Carlos, unpublished data).

Here, we tested a novel chemical ERK1/2 inhibitor, SCH772984, recently released by Merck, for its potential to selectively eliminate cells with compromised capacity of recombinational repair. Structural analyses demonstrated that SCH772984 binds to the catalytic pocket of ERK1/2 in an unconventional manner inducing a conformational distortion, which accounts for the slow off-rate and unprecedented specificity of this compound (Chaikuad *et al.*, 2014). Treatment with SCH772984 resulted in a dose-dependent proliferative arrest of BRCA2- and RAD51-depleted HEK-293T cells (Figure 4 & Figure 5). This effect was less pronounced in cells treated with BRCA2 siRNA, probably due to the fact that siRNA-mediated depletion is unsuitable for maintaining sufficiently low levels of BRCA2 for the entire duration of the assay (six days). However, treatment of V-C8 hamster cells with SCH772984 lacking BRCA2 led to significant toxicity compared to control BRCA2-complemented cells (Chaikuad *et al.*, 2014). A similar anti-proliferative effect was observed after treatment with the previously described ERK1/2 inhibitor VTX-11e (Aronov *et al.*, 2009) (Figure 4 & Figure

5). These results indicate that HR-deficient cells rely on the pro-proliferative functions of the MAPK pathway (Xia *et al.*, 1995; Yujiri *et al.*, 1998) to survive, even in the absence of p53. The mechanism that determines this specificity over other survival pathways remains unknown.

Overall, our findings are in agreement with previous results suggesting that ERK1/2 are favourable targets for efficient and selective elimination of HR-deficient tumours (Carlos *et al.*, 2013). In addition, this study reports the potential of SCH772984 as a novel therapeutic compound.

4.2 G4 stabilisation is deleterious to HR-deficient cells

Therapeutic approaches for targeting HR-deficient tumours include DNA-damaging radio- and/or chemotherapy. This strategy is based on the error-prone and/or compromised repair of DNA damage in the absence of HR. Since G4s have the potential to act as replication fork barriers (Lopes *et al.*, 2011; Paeschke *et al.*, 2011; Ribeyre *et al.*, 2009), and HR is required for restart and repair of stalled replication forks (Lomonosov *et al.*, 2003; Nagaraju *et al.*, 2007), we hypothesised that stabilisation of G4s might be less tolerated by and thus allow for selective targeting of HR-deficient cells. We detected a significant decrease in the viability of HR-defective cells after treatment with two different G4 stabilisers (Figure 6, Figure 7 & Figure 8). Importantly, the proliferative capacity of HR-proficient cells remained mostly unaffected (Figure 6, Figure 7 & Figure 8). The differences observed in the efficiency of pyridostatin and $PhenDC_3$ relative to each other may reflect differences in cell permeation and subcellular localisation of each compound.

We observed that pyridostatin and $PhenDC_3$ induced elevated expression levels of the DNA damage marker γH2AX and the apoptosis marker cleaved PARP in cells lacking HR capacity (Figure 9). In line with our hypothesis, these findings indicate that G4 stabilisation induces DNA damage and promotes apoptosis of HR-deficient cells. Previous studies have established that HR abrogation triggers accumulation of replication-associated DSBs (Arnaudeau *et al.*, 2001). Pyridostatin treatment was reported to have the same effect in cultured cells (Rodriguez *et al.*, 2012). Consistent with this, comet assays revealed accumulation of DNA damage in cells lacking RAD51 and also in cells exposed to pyridostatin regardless of their HR capacity (Figure 10). Nonetheless, pyridostatin treatment triggered a substantial and statistically significant increase in DNA damage in HR-deficient cells (Figure 10). Quantification of γH2AX foci formation using immunofluorescence staining (Figure 11) and of DSBs using mitotic chromosome spreads (Figure 12) similarly demonstrated a significant enhancement of DNA damage levels in HR-deficient cells upon treatment with pyridostatin. It is important to note that the majority of HR-deficient cells treated with pyridostatin accumulate in G2/M phase (Figure 14). It is therefore conceivable that the mitotic DSB quantification reflect only the subset of cells that escaped this block, whilst cells with very high levels of DNA damage were most likely excluded from this analysis. Overall, our study demonstrates that the DNA-damaging effect of G4 stabilisation previously reported in a variety of cell lines (Rodriguez *et al.*, 2012; Rodriguez *et al.*, 2008) is less tolerated by HR-compromised cells, which already carry significant levels of DSBs, ultimately triggering genomic instability and cell death.

G4 stabilisation caused activation of the ATM- and ATR-dependent cell cycle checkpoints (Figure 13) and G2/M cell cycle arrest (Figure 14) in HR-deficient cells.

Together, these results corroborate the observed DNA damage accumulation and provide an explanation for the reduced proliferation rate of these cells. Elevated RPA expression levels (Figure 13) and RPA foci assembly (Figure 15) are indicative of acute replication stress elicited by persistent G4s. Furthermore, the slow replication fork progression detected in DNA fibre assays (Figure 16b) provided compelling evidence that replication stress is a major factor of G4 stabiliser-triggered toxicity in HR-deficient cells. Stalling of replication forks and reduced DNA synthesis define replication stress (Zeman *et al.*, 2014), which in turn leads to firing of dormant origins (Ge *et al.*, 2010; Ibarra *et al.*, 2008; Woodward *et al.*, 2006). All of these characteristics of replication stress were observed in pyridostatin-treated cells (Figure 16), consistent with recent studies showing that G4 stabilisation interferes with replication (Lopes *et al.*, 2011; Rodriguez *et al.*, 2012). Loss of RAD51 also caused the mentioned symptoms of replication stress (Figure 16), in line with the previously reported requirement for RAD51 in the restart and repair of stalled replication forks (Petermann *et al.*, 2010). Importantly, however, pyridostatin had an additive effect on RAD51 abrogation in obstructing replication fork progression (Figure 16b), which demonstrates that HR-deficient cells are highly susceptible to the additional replication stress induced by G4 stabilisation. Cumulative replication defects may explain why G4-stabilising compounds are particularly deleterious to cells whose capacity of HR repair has been compromised.

Approximately 40% of promoters in the human genome are predicted to display G4 motifs suggesting a functional role in transcriptional regulation (Huppert *et al.*, 2005). This led us to investigate the effect of pyridostatin on the transcription levels of genes with high content of G4-forming sequences (*MYC*, *SRC*, *SREBF1*), as predicted by

the QGRS Mapper (Kikin *et al.*, 2006), using RT-qPCR. A statistically significant decrease in the transcription levels of all three genes was observed after treatment with pyridostatin regardless of the HR status (Figure 17). This finding is consistent with previous studies demonstrating that G4 stabilisation triggers changes in the transcriptome with specific alterations in the transcription profile of G4-containing genes (Halder *et al.*, 2012; Rodriguez *et al.*, 2012). It is possible that G4 stabilisation leads to replication fork stalling and subsequent DNA damage at sites with high G4-forming potential. This in turn could cause reduced mRNA levels because DNA lesions within a genomic locus can inhibit transcription in *cis* (Shanbhag *et al.*, 2010) or because the transcription machinery is unable to pass the lesions. In this study, we report that HR deficiency has an additive effect on the DNA-damaging potential of G4 stabilisation. Whether the G4 stabilisers used in this study function through inducing DNA damage *per se* or act as physical barriers obstructing access to transcription machineries, remains to be elucidated. It is also possible that these drugs exert a combination of both effects, as physical data show that pyridostatin-mediated G4 stabilisation enables resistance of these structures to the mechanical forces applied by either DNA or RNA polymerases (Koirala *et al.*, 2011). DNA exposure to the even higher physical forces induced by chromatin remodelling during active transcription and replication conceivably results in breakage. Additionally, endonucleases have been proposed to mediate the DNA-damaging effect of G4-interacting compounds (Rodriguez *et al.*, 2012). In this respect, it is possible that the effect of pyridostatin on transcription is mechanistically similar to transcription-coupled repair poisoning previously reported for the anti-cancer drug ecteinascidin 743 (Takebayashi *et al.*, 2001).

Finally, we used SV40-derived plasmids to measure the replication efficiency of G4-forming sequences upon transfection into human cells (Figure 18). We detected no difference in the replication efficiencies of these sequences when HR was abrogated compared to control cells. We assign this negative result to the limitations of the assay, most likely to the high processivity of the SV40 helicase, which may enable replication through secondary structures difficult to bypass by the cellular replication machinery. Further arguing against the possibility that HR is not required for efficient G4 replication are recent results from our laboratory using a plasmid-based replication assay, in which the conventional replication machinery is recruited to the origin of replication through artificial tethering mediated by CDC6 (Szüts *et al.*, 2008). Using this system, we established that the replication efficiency of telomeric repeats is significantly decreased in cells lacking the HR activities of BRCA2 or RAD51C (E. Tacconi, unpublished data). In addition, chromosome-orientation FISH (CO-FISH) assays proved that replication of the G-rich telomeric strand with G-forming potential is significantly reduced when HR is genetically abrogated (E. Tacconi, K. Klare, unpublished data). These results strongly support the requirement of HR reactions for G4 replication, possibly to rescue stalled replication forks or to repair DNA breaks introduced in the vicinity of G4s (Tarsounas *et al.*, 2013).

4.3 Conclusions

In summary, we report here that the ERK1/2 inhibitors SCH772984 and VTX-11e exert significant anti-proliferative effects, which are specific for HR deficiency, thereby confirming ERK1/2 as potential targets for anti-cancer therapy of HR-deficient

tumours. Further *in vivo* experimentation is required to establish the suitability of these compounds for clinical applications.

In addition, our study highlights the therapeutic potential of G4 stabilisation in the context of HR deficiency. We show that chemical compounds that bind and stabilise G4s also generate DNA damage and replication stress leading to reduced cell proliferation and apoptosis in cells lacking HR activities. This supports the notion that HR-compromised cells are vulnerable to G4-driven genomic instability and identifies G4 stabilisers, in particular pyridostatin, as anti-cancer agents with therapeutic potential particularly relevant to HR-deficient tumours.

5 References

Arnaudeau, C., Lundin, C. and Helleday, T. 2001. DNA double-strand breaks associated with replication forks are predominantly repaired by homologous recombination involving an exchange mechanism in mammalian cells. *Journal of molecular biology*. 307:1235-1245.

Aronov, A. M., Tang, Q., Martinez-Botella, G., Bemis, G. W., Cao, J., Chen, G., Ewing, N. P., Ford, P. J., Germann, U. A., Green, J., Hale, M. R., Jacobs, M., Janetka, J. W., Maltais, F., Markland, W., Namchuk, M. N., Nanthakumar, S., Poondru, S., Straub, J., ter Haar, E. and Xie, X. 2009. Structure-guided design of potent and selective pyrimidylpyrrole inhibitors of extracellular signal-regulated kinase (ERK) using conformational control. *Journal of medicinal chemistry*. 52:6362-6368.

Audeh, M. W., Carmichael, J., Penson, R. T., Friedlander, M., Powell, B., Bell-McGuinn, K. M., Scott, C., Weitzel, J. N., Oaknin, A., Loman, N., Lu, K., Schmutzler, R. K., Matulonis, U., Wickens, M. and Tutt, A. 2010. Oral poly(ADP-ribose) polymerase inhibitor olaparib in patients with *BRCA1* or *BRCA2* mutations and recurrent ovarian cancer: a proof-of-concept trial. *Lancet*. 376:245-251.

Badie, S., Escandell, J. M., Bouwman, P., Carlos, A. R., Thanasoula, M., Gallardo, M. M., Suram, A., Jaco, I., Benitez, J., Herbig, U., Blasco, M. A., Jonkers, J. and Tarsounas, M. 2010. BRCA2 acts as a RAD51 loader to facilitate telomere replication and capping. *Nature structural & molecular biology*. 17:1461-1469.

Ban, S., Shinohara, T., Hirai, Y., Moritaku, Y., Cologne, J. B. and MacPhee, D. G. 2001. Chromosomal instability in BRCA1- or BRCA2-defective human cancer cells detected by spontaneous micronucleus assay. *Mutation research*. 474:15-23.

Barber, L. J., Sandhu, S., Chen, L., Campbell, J., Kozarewa, I., Fenwick, K., Assiotis, I., Rodrigues, D. N., Reis Filho, J. S., Moreno, V., Mateo, J., Molife, L. R., De Bono, J., Kaye, S., Lord, C. J. and Ashworth, A. 2013. Secondary mutations in *BRCA2* associated with clinical resistance to a PARP inhibitor. *The Journal of pathology*. 229:422-429.

Baumann, P., Benson, F. E. and West, S. C. 1996. Human Rad51 protein promotes ATP-dependent homologous pairing and strand transfer reactions in vitro. *Cell*. 87:757-766.

Benson, F. E., Stasiak, A. and West, S. C. 1994. Purification and characterization of the human Rad51 protein, an analogue of *E. coli* RecA. *The EMBO journal*. 13:5764-5771.

Besnard, E., Babled, A., Lapasset, L., Milhavet, O., Parrinello, H., Dantec, C., Marin, J. M. and Lemaitre, J. M. 2012. Unraveling cell type-specific and reprogrammable human replication origin signatures associated with G-quadruplex consensus motifs. *Nature structural & molecular biology*. 19:837-844.

Bianchi, V., Pontis, E. and Reichard, P. 1986. Changes of deoxyribonucleoside triphosphate pools induced by hydroxyurea and their relation to DNA synthesis. *The Journal of biological chemistry*. 261:16037-16042.

Biffi, G., Tannahill, D., McCafferty, J. and Balasubramanian, S. 2013. Quantitative visualization of DNA G-quadruplex structures in human cells. *Nature chemistry*. 5:182-186.

Bishop, D. K., Ear, U., Bhattacharyya, A., Calderone, C., Beckett, M., Weichselbaum, R. R. and Shinohara, A. 1998. Xrcc3 is required for assembly of Rad51 complexes *in vivo*. *The Journal of biological chemistry*. 273:21482-21488.

Blackburn, E. H. 2001. Switching and signaling at the telomere. *Cell*. 106:661-673.

Bothmer, A., Robbiani, D. F., Feldhahn, N., Gazumyan, A., Nussenzweig, A. and Nussenzweig, M. C. 2010. 53BP1 regulates DNA resection and the choice between classical and alternative end joining during class switch recombination. *The Journal of experimental medicine*. 207:855-865.

Bouwman, P., Aly, A., Escandell, J. M., Pieterse, M., Bartkova, J., van der Gulden, H., Hiddingh, S., Thanasoula, M., Kulkarni, A., Yang, Q., Haffty, B. G., Tommiska, J., Blomqvist, C.,

Drapkin, R., Adams, D. J., Nevanlinna, H., Bartek, J., Tarsounas, M., Ganesan, S. and Jonkers, J. 2010. 53BP1 loss rescues BRCA1 deficiency and is associated with triple-negative and BRCA-mutated breast cancers. *Nature structural & molecular biology*. 17:688-695.

Brown, A. L., Lee, C. H., Schwarz, J. K., Mitiku, N., Piwnica-Worms, H. and Chung, J. H. 1999. A human Cds1-related kinase that functions downstream of ATM protein in the cellular response to DNA damage. *Proceedings of the National Academy of Sciences of the United States of America*. 96:3745-3750.

Bruchim, I., Fishman, A., Friedman, E., Goldberg, I., Chetrit, A., Barshack, I., Dekel, E., Hirsh-Yechezkel, G., Modan, B. and Kopolovic, J. 2004. Analyses of p53 expression pattern and BRCA mutations in patients with double primary breast and ovarian cancer. *International journal of gynecological cancer : official journal of the International Gynecological Cancer Society*. 14:251-258.

Bryant, H. E., Schultz, N., Thomas, H. D., Parker, K. M., Flower, D., Lopez, E., Kyle, S., Meuth, M., Curtin, N. J. and Helleday, T. 2005. Specific killing of BRCA2-deficient tumours with inhibitors of poly(ADP-ribose) polymerase. *Nature*. 434:913-917.

Bunting, S. F., Callen, E., Wong, N., Chen, H. T., Polato, F., Gunn, A., Bothmer, A., Feldhahn, N., Fernandez-Capetillo, O., Cao, L., Xu, X., Deng, C. X., Finkel, T., Nussenzweig, M., Stark, J. M. and Nussenzweig, A. 2010. 53BP1 inhibits homologous recombination in *Brca1*-deficient cells by blocking resection of DNA breaks. *Cell*. 141:243-254.

Cahoon, L. A. and Seifert, H. S. 2009. An alternative DNA structure is necessary for pilin antigenic variation in *Neisseria gonorrhoeae*. *Science*. 325:764-767.

Cao, L., Xu, X., Bunting, S. F., Liu, J., Wang, R. H., Cao, L. L., Wu, J. J., Peng, T. N., Chen, J., Nussenzweig, A., Deng, C. X. and Finkel, T. 2009. A selective requirement for 53BP1 in the biological response to genomic instability induced by Brca1 deficiency. *Molecular cell*. 35:534-541.

Carlos, A. R., Escandell, J. M., Kotsantis, P., Suwaki, N., Bouwman, P., Badie, S., Folio, C., Benitez, J., Gomez-Lopez, G., Pisano, D. G., Jonkers, J. and Tarsounas, M. 2013. ARF triggers senescence in *Brca2*-deficient cells by altering the spectrum of p53 transcriptional targets. *Nature communications*. 4:2697.

Cerbinskaite, A., Mukhopadhyay, A., Plummer, E. R., Curtin, N. J. and Edmondson, R. J. 2012. Defective homologous recombination in human cancers. *Cancer treatment reviews*. 38:89-100.

Cesare, A. J. and Reddel, R. R. 2008. Telomere uncapping and alternative lengthening of telomeres. *Mechanisms of ageing and development*. 129:99-108.

Chaikuad, A., E, M. C. T., Zimmer, J., Liang, Y., Gray, N. S., Tarsounas, M. and Knapp, S. 2014. A unique inhibitor binding site in ERK1/2 is associated with slow binding kinetics. *Nature chemical biology*. 10:853-860.

Chapman, J. R., Taylor, M. R. and Boulton, S. J. 2012. Playing the end game: DNA double-strand break repair pathway choice. *Molecular cell*. 47:497-510.

Chaturvedi, P., Eng, W. K., Zhu, Y., Mattern, M. R., Mishra, R., Hurle, M. R., Zhang, X., Annan, R. S., Lu, Q., Faucette, L. F., Scott, G. F., Li, X., Carr, S. A., Johnson, R. K., Winkler, J. D. and Zhou, B. B. 1999. Mammalian Chk2 is a downstream effector of the ATM-dependent DNA damage checkpoint pathway. *Oncogene*. 18:4047-4054.

Chen, H., Lisby, M. and Symington, L. S. 2013. RPA coordinates DNA end resection and prevents formation of DNA hairpins. *Molecular cell*. 50:589-600.

Chen, Z., Gibson, T. B., Robinson, F., Silvestro, L., Pearson, G., Xu, B., Wright, A., Vanderbilt, C. and Cobb, M. H. 2001. MAP kinases. *Chemical reviews*. 101:2449-2476.

Chiarugi, A. 2012. A snapshot of chemoresistance to PARP inhibitors. *Trends in pharmacological sciences*. 33:42-48.

Costanzo, V., Shechter, D., Lupardus, P. J., Cimprich, K. A., Gottesman, M. and Gautier, J. 2003. An ATR- and Cdc7-dependent DNA damage checkpoint that inhibits initiation of DNA replication. *Molecular cell*. 11:203-213.

Daboussi, F., Courbet, S., Benhamou, S., Kannouche, P., Zdzienicka, M. Z., Debatisse, M. and Lopez, B. S. 2008. A homologous recombination defect affects replication-fork progression in mammalian cells. *Journal of cell science*. 121:162-166.

Dasari, S. and Bernard Tchounwou, P. 2014. Cisplatin in cancer therapy: Molecular mechanisms of action. *European journal of pharmacology*.

De Cian, A., Delemos, E., Mergny, J. L., Teulade-Fichou, M. P. and Monchaud, D. 2007. Highly efficient G-quadruplex recognition by bisquinolinium compounds. *Journal of the American Chemical Society*. 129:1856-1857.

De, S. and Michor, F. 2011. DNA secondary structures and epigenetic determinants of cancer genome evolution. *Nature structural & molecular biology*. 18:950-955.

Denchi, E. L. and de Lange, T. 2007. Protection of telomeres through independent control of ATM and ATR by TRF2 and POT1. *Nature*. 448:1068-1071.

Dhillon, A. S., Hagan, S., Rath, O. and Kolch, W. 2007. MAP kinase signalling pathways in cancer. *Oncogene*. 26:3279-3290.

Dobzhansky, T. 1946. Genetics of Natural Populations. Xiii. Recombination and Variability in Populations of *Drosophila Pseudoobscura*. *Genetics*. 31:269-290.

Duquette, M. L., Handa, P., Vincent, J. A., Taylor, A. F. and Maizels, N. 2004. Intracellular transcription of G-rich DNAs induces formation of G-loops, novel structures containing G4 DNA. *Genes & development*. 18:1618-1629.

Dynan, W. S. and Yoo, S. 1998. Interaction of Ku protein and DNA-dependent protein kinase catalytic subunit with nucleic acids. *Nucleic acids research*. 26:1551-1559.

Eddy, S., Ketkar, A., Zafar, M. K., Maddukuri, L., Choi, J. Y. and Eoff, R. L. 2014. Human Rev1 polymerase disrupts G-quadruplex DNA. *Nucleic acids research*. 42:3272-3285.

Edwards, S. L., Brough, R., Lord, C. J., Natrajan, R., Vatcheva, R., Levine, D. A., Boyd, J., Reis-Filho, J. S. and Ashworth, A. 2008. Resistance to therapy caused by intragenic deletion in *BRCA2*. *Nature*. 451:1111-1115.

Fanning, E., Klimovich, V. and Nager, A. R. 2006. A dynamic model for replication protein A (RPA) function in DNA processing pathways. *Nucleic acids research*. 34:4126-4137.

Fanning, E. and Zhao, K. 2009. SV40 DNA replication: from the A gene to a nanomachine. *Virology*. 384:352-359.

Farmer, H., McCabe, N., Lord, C. J., Tutt, A. N., Johnson, D. A., Richardson, T. B., Santarosa, M., Dillon, K. J., Hickson, I., Knights, C., Martin, N. M., Jackson, S. P., Smith, G. C. and Ashworth, A. 2005. Targeting the DNA repair defect in *BRCA* mutant cells as a therapeutic strategy. *Nature*. 434:917-921.

Feng, Z. and Zhang, J. 2012. A dual role of BRCA1 in two distinct homologous recombination mediated repair in response to replication arrest. *Nucleic acids research*. 40:726-738.

Follonier, C. and Lopes, M. 2014. Combined bidimensional electrophoresis and electron microscopy to study specific plasmid DNA replication intermediates in human cells. *Methods in molecular biology*. 1094:209-219.

Fong, P. C., Boss, D. S., Yap, T. A., Tutt, A., Wu, P., Mergui-Roelvink, M., Mortimer, P., Swaisland, H., Lau, A., O'Connor, M. J., Ashworth, A., Carmichael, J., Kaye, S. B., Schellens, J. H. and de Bono, J. S. 2009. Inhibition of poly(ADP-ribose) polymerase in tumors from *BRCA* mutation carriers. *The New England journal of medicine*. 361:123-134.

Fry, M. and Loeb, L. A. 1999. Human werner syndrome DNA helicase unwinds tetrahelical structures of the fragile X syndrome repeat sequence d(CGG)n. *The Journal of biological chemistry*. 274:12797-12802.

Ge, X. Q. and Blow, J. J. 2010. Chk1 inhibits replication factory activation but allows dormant origin firing in existing factories. *The Journal of cell biology*. 191:1285-1297.

Gellert, M., Lipsett, M. N. and Davies, D. R. 1962. Helix formation by guanylic acid. *Proceedings of the National Academy of Sciences of the United States of America*. 48:2013-2018.

Gomez, D., Guedin, A., Mergny, J. L., Salles, B., Riou, J. F., Teulade-Fichou, M. P. and Calsou, P. 2010. A G-quadruplex structure within the 5'-UTR of TRF2 mRNA represses translation in human cells. *Nucleic acids research*. 38:7187-7198.

Gretarsdottir, S., Thorlacius, S., Valgardsdottir, R., Gudlaugsdottir, S., Sigurdsson, S., Steinarsdottir, M., Jonasson, J. G., Anamthawat-Jonsson, K. and Eyfjord, J. E. 1998. BRCA2 and p53 mutations in primary breast cancer in relation to genetic instability. *Cancer research*. 58:859-862.

Hakem, R., de la Pompa, J. L., Sirard, C., Mo, R., Woo, M., Hakem, A., Wakeham, A., Potter, J., Reitmair, A., Billia, F., Firpo, E., Hui, C. C., Roberts, J., Rossant, J. and Mak, T. W. 1996. The tumor suppressor gene *Brca1* is required for embryonic cellular proliferation in the mouse. *Cell*. 85:1009-1023.

Halder, K., Largy, E., Benzler, M., Teulade-Fichou, M. P. and Hartig, J. S. 2011. Efficient suppression of gene expression by targeting 5'-UTR-based RNA quadruplexes with bisquinolinium compounds. *Chembiochem : a European journal of chemical biology*. 12:1663-1668.

Halder, R., Riou, J. F., Teulade-Fichou, M. P., Frickey, T. and Hartig, J. S. 2012. Bisquinolinium compounds induce quadruplex-specific transcriptome changes in HeLa S3 cell lines. *BMC research notes*. 5:138.

Hanahan, D. and Weinberg, R. A. 2011. Hallmarks of cancer: the next generation. *Cell*. 144:646-674.

Hartlerode, A. J. and Scully, R. 2009. Mechanisms of double-strand break repair in somatic mammalian cells. *The Biochemical journal*. 423:157-168.

Henry-Mowatt, J., Jackson, D., Masson, J. Y., Johnson, P. A., Clements, P. M., Benson, F. E., Thompson, L. H., Takeda, S., West, S. C. and Caldecott, K. W. 2003. XRCC3 and Rad51 modulate replication fork progression on damaged vertebrate chromosomes. *Molecular cell*. 11:1109-1117.

Henson, J. D., Neumann, A. A., Yeager, T. R. and Reddel, R. R. 2002. Alternative lengthening of telomeres in mammalian cells. *Oncogene*. 21:598-610.

Heyer, W. D., Ehmsen, K. T. and Liu, J. 2010. Regulation of homologous recombination in eukaryotes. *Annual review of genetics*. 44:113-139.

Huber, M. D., Lee, D. C. and Maizels, N. 2002. G4 DNA unwinding by BLM and Sgs1p: substrate specificity and substrate-specific inhibition. *Nucleic acids research*. 30:3954-3961.

Huppert, J. L. and Balasubramanian, S. 2005. Prevalence of quadruplexes in the human genome. *Nucleic acids research*. 33:2908-2916.

Ibarra, A., Schwob, E. and Mendez, J. 2008. Excess MCM proteins protect human cells from replicative stress by licensing backup origins of replication. *Proceedings of the National Academy of Sciences of the United States of America*. 105:8956-8961.

Ikegami, S., Taguchi, T., Ohashi, M., Oguro, M., Nagano, H. and Mano, Y. 1978. Aphidicolin prevents mitotic cell division by interfering with the activity of DNA polymerase-alpha. *Nature*. 275:458-460.

Johnson, R. D. and Jasin, M. 2000. Sister chromatid gene conversion is a prominent double-strand break repair pathway in mammalian cells. *The EMBO journal*. 19:3398-3407.

Johnson, R. D., Liu, N. and Jasin, M. 1999. Mammalian XRCC2 promotes the repair of DNA double-strand breaks by homologous recombination. *Nature*. 401:397-399.

Kikin, O., D'Antonio, L. and Bagga, P. S. 2006. QGRS Mapper: a web-based server for predicting G-quadruplexes in nucleotide sequences. *Nucleic acids research*. 34:W676-682.

King, M. C., Marks, J. H., Mandell, J. B. and New York Breast Cancer Study, G. 2003. Breast and ovarian cancer risks due to inherited mutations in *BRCA1* and *BRCA2*. *Science*. 302:643-646.

Koirala, D., Dhakal, S., Ashbridge, B., Sannohe, Y., Rodriguez, R., Sugiyama, H., Balasubramanian, S. and Mao, H. 2011. A single-molecule platform for investigation of interactions between G-quadruplexes and small-molecule ligands. *Nature chemistry*. 3:782-787.

Kraakman-van der Zwet, M., Overkamp, W. J., van Lange, R. E., Essers, J., van Duijn-Goedhart, A., Wiggers, I., Swaminathan, S., van Buul, P. P., Errami, A., Tan, R. T., Jaspers, N. G., Sharan, S. K., Kanaar, R. and Zdzienicka, M. Z. 2002. Brca2 (XRCC11) deficiency results in radioresistant DNA synthesis and a higher frequency of spontaneous deletions. *Molecular and cellular biology*. 22:669-679.

Kruisselbrink, E., Guryev, V., Brouwer, K., Pontier, D. B., Cuppen, E. and Tijsterman, M. 2008. Mutagenic capacity of endogenous G4 DNA underlies genome instability in FANCJ-defective *C. elegans*. *Current biology : CB*. 18:900-905.

Lam, E. Y., Beraldi, D., Tannahill, D. and Balasubramanian, S. 2013. G-quadruplex structures are stable and detectable in human genomic DNA. *Nature communications*. 4:1796.

Li, J., Zou, C., Bai, Y., Wazer, D. E., Band, V. and Gao, Q. 2006. DSS1 is required for the stability of BRCA2. *Oncogene*. 25:1186-1194.

Liu, Q., Guntuku, S., Cui, X. S., Matsuoka, S., Cortez, D., Tamai, K., Luo, G., Carattini-Rivera, S., DeMayo, F., Bradley, A., Donehower, L. A. and Elledge, S. J. 2000. Chk1 is an essential kinase that is regulated by Atr and required for the G(2)/M DNA damage checkpoint. *Genes & development*. 14:1448-1459.

Liu, X., Han, E. K., Anderson, M., Shi, Y., Semizarov, D., Wang, G., McGonigal, T., Roberts, L., Lasko, L., Palma, J., Zhu, G. D., Penning, T., Rosenberg, S., Giranda, V. L., Luo, Y., Leverson, J., Johnson, E. F. and Shoemaker, A. R. 2009. Acquired resistance to combination treatment with temozolomide and ABT-888 is mediated by both base excision repair and homologous recombination DNA repair pathways. *Molecular cancer research : MCR*. 7:1686-1692.

Lodish, H., Berk, A., Matsudaira, P., Kaiser, C. A., Krieger, M., Scott, M. P., Zipursky, S. L. and Darnell, J. 2004. Molecular Cell Biology. W. H. Freeman, New York.

Lomonosov, M., Anand, S., Sangrithi, M., Davies, R. and Venkitaraman, A. R. 2003. Stabilization of stalled DNA replication forks by the BRCA2 breast cancer susceptibility protein. *Genes & development*. 17:3017-3022.

London, T. B., Barber, L. J., Mosedale, G., Kelly, G. P., Balasubramanian, S., Hickson, I. D., Boulton, S. J. and Hiom, K. 2008. FANCJ is a structure-specific DNA helicase associated with the maintenance of genomic G/C tracts. *The Journal of biological chemistry*. 283:36132-36139.

Lopes, J., Piazza, A., Bermejo, R., Kriegsman, B., Colosio, A., Teulade-Fichou, M. P., Foiani, M. and Nicolas, A. 2011. G-quadruplex-induced instability during leading-strand replication. *The EMBO journal*. 30:4033-4046.

Lopez-Girona, A., Tanaka, K., Chen, X. B., Baber, B. A., McGowan, C. H. and Russell, P. 2001. Serine-345 is required for Rad3-dependent phosphorylation and function of checkpoint kinase Chk1 in fission yeast. *Proceedings of the National Academy of Sciences of the United States of America*. 98:11289-11294.

Lord, C. J. and Ashworth, A. 2012. The DNA damage response and cancer therapy. *Nature*. 481:287-294.

Loveday, C., Turnbull, C., Ruark, E., Xicola, R. M., Ramsay, E., Hughes, D., Warren-Perry, M., Snape, K., Breast Cancer Susceptibility, C., Eccles, D., Evans, D. G., Gore, M., Renwick, A., Seal, S., Antoniou, A. C. and Rahman, N. 2012. Germline *RAD51C* mutations confer susceptibility to ovarian cancer. *Nature genetics*. 44:475-476; author reply 476.

Lukas, J., Lukas, C. and Bartek, J. 2011. More than just a focus: The chromatin response to DNA damage and its role in genome integrity maintenance. *Nature cell biology*. 13:1161-1169.

Marechal, A. and Zou, L. 2013. DNA damage sensing by the ATM and ATR kinases. *Cold Spring Harbor perspectives in biology*. 5.

Matsuoka, S., Huang, M. and Elledge, S. J. 1998. Linkage of ATM to cell cycle regulation by the Chk2 protein kinase. *Science*. 282:1893-1897.

McCabe, N., Turner, N. C., Lord, C. J., Kluzek, K., Bialkowska, A., Swift, S., Giavara, S., O'Connor, M. J., Tutt, A. N., Zdzienicka, M. Z., Smith, G. C. and Ashworth, A. 2006. Deficiency in the repair of DNA damage by homologous recombination and sensitivity to poly(ADP-ribose) polymerase inhibition. *Cancer research*. 66:8109-8115.

McClintock, B. 1941. The Stability of Broken Ends of Chromosomes in *Zea Mays*. *Genetics*. 26:234-282.

Mechali, M. 2010. Eukaryotic DNA replication origins: many choices for appropriate answers. *Nature reviews. Molecular cell biology*. 11:728-738.

Mechali, M., Yoshida, K., Coulombe, P. and Pasero, P. 2013. Genetic and epigenetic determinants of DNA replication origins, position and activation. *Current opinion in genetics & development*. 23:124-131.

Meindl, A., Hellebrand, H., Wiek, C., Erven, V., Wappenschmidt, B., Niederacher, D., Freund, M., Lichtner, P., Hartmann, L., Schaal, H., Ramser, J., Honisch, E., Kubisch, C., Wichmann, H. E., Kast, K., Deissler, H., Engel, C., Muller-Myhsok, B., Neveling, K., Kiechle, M., Mathew, C. G., Schindler, D., Schmutzler, R. K. and Hanenberg, H. 2010. Germline mutations in breast and ovarian cancer pedigrees establish *RAD51C* as a human cancer susceptibility gene. *Nature genetics*. 42:410-414.

Meyne, J., Ratliff, R. L. and Moyzis, R. K. 1989. Conservation of the human telomere sequence (TTAGGG)n among vertebrates. *Proceedings of the National Academy of Sciences of the United States of America*. 86:7049-7053.

Mimitou, E. P. and Symington, L. S. 2011. DNA end resection--unraveling the tail. *DNA repair*. 10:344-348.

Mohaghegh, P., Karow, J. K., Brosh, R. M., Jr., Bohr, V. A. and Hickson, I. D. 2001. The Bloom's and Werner's syndrome proteins are DNA structure-specific helicases. *Nucleic acids research*. 29:2843-2849.

Monchaud, D., Allain, C., Bertrand, H., Smargiasso, N., Rosu, F., Gabelica, V., De Cian, A., Mergny, J. L. and Teulade-Fichou, M. P. 2008. Ligands playing musical chairs with G-quadruplex DNA: a rapid and simple displacement assay for identifying selective G-quadruplex binders. *Biochimie*. 90:1207-1223.

Morris, E. J., Jha, S., Restaino, C. R., Dayananth, P., Zhu, H., Cooper, A., Carr, D., Deng, Y., Jin, W., Black, S., Long, B., Liu, J., Dinunzio, E., Windsor, W., Zhang, R., Zhao, S., Angagaw, M. H., Pinheiro, E. M., Desai, J., Xiao, L., Shipps, G., Hruza, A., Wang, J., Kelly, J., Paliwal, S., Gao, X., Babu, B. S., Zhu, L., Daublain, P., Zhang, L., Lutterbach, B. A., Pelletier, M. R., Philippar, U., Siliphaivanh, P., Witter, D., Kirschmeier, P., Bishop, W. R., Hicklin, D., Gilliland, D. G., Jayaraman, L., Zawel, L., Fawell, S. and Samatar, A. A. 2013. Discovery of a novel ERK inhibitor with activity in models of acquired resistance to BRAF and MEK inhibitors. *Cancer discovery*. 3:742-750.

Moynahan, M. E., Pierce, A. J. and Jasin, M. 2001. BRCA2 is required for homology-directed repair of chromosomal breaks. *Molecular cell*. 7:263-272.

Moyzis, R. K., Buckingham, J. M., Cram, L. S., Dani, M., Deaven, L. L., Jones, M. D., Meyne, J., Ratliff, R. L. and Wu, J. R. 1988. A highly conserved repetitive DNA sequence, (TTAGGG)n, present at the telomeres of human chromosomes. *Proceedings of the National Academy of Sciences of the United States of America*. 85:6622-6626.

Müller, S., Kumari, S., Rodriguez, R. and Balasubramanian, S. 2010. Small-molecule-mediated G-quadruplex isolation from human cells. *Nature chemistry*. 2:1095-1098.

Nagaraju, G. and Scully, R. 2007. Minding the gap: the underground functions of BRCA1 and BRCA2 at stalled replication forks. *DNA repair*. 6:1018-1031.

Nam, E. A. and Cortez, D. 2011. ATR signalling: more than meeting at the fork. *The Biochemical journal*. 436:527-536.

Negrini, S., Gorgoulis, V. G. and Halazonetis, T. D. 2010. Genomic instability--an evolving hallmark of cancer. *Nature reviews. Molecular cell biology*. 11:220-228.

Nimonkar, A. V., Genschel, J., Kinoshita, E., Polaczek, P., Campbell, J. L., Wyman, C., Modrich, P. and Kowalczykowski, S. C. 2011. BLM-DNA2-RPA-MRN and EXO1-BLM-RPA-MRN constitute two DNA end resection machineries for human DNA break repair. *Genes & development*. 25:350-362.

Nimonkar, A. V., Ozsoy, A. Z., Genschel, J., Modrich, P. and Kowalczykowski, S. C. 2008. Human exonuclease 1 and BLM helicase interact to resect DNA and initiate DNA repair. *Proceedings of the National Academy of Sciences of the United States of America*. 105:16906-16911.

Oliver, F. J., de la Rubia, G., Rolli, V., Ruiz-Ruiz, M. C., de Murcia, G. and Murcia, J. M. 1998. Importance of poly(ADP-ribose) polymerase and its cleavage in apoptosis. Lesson from an uncleavable mutant. *The Journal of biological chemistry*. 273:33533-33539.

Paeschke, K., Capra, J. A. and Zakian, V. A. 2011. DNA replication through G-quadruplex motifs is promoted by the *Saccharomyces cerevisiae* Pif1 DNA helicase. *Cell*. 145:678-691.

Palm, W. and de Lange, T. 2008. How shelterin protects mammalian telomeres. *Annual review of genetics*. 42:301-334.

Pan, S. S., Iracki, T. and Bachur, N. R. 1986. DNA alkylation by enzyme-activated mitomycin C. *Molecular pharmacology*. 29:622-628.

Parkinson, G. N., Lee, M. P. and Neidle, S. 2002. Crystal structure of parallel quadruplexes from human telomeric DNA. *Nature*. 417:876-880.

Parsons, J. L., Tait, P. S., Finch, D., Dianova, II, Edelmann, M. J., Khoronenkova, S. V., Kessler, B. M., Sharma, R. A., McKenna, W. G. and Dianov, G. L. 2009. Ubiquitin ligase ARF-BP1/Mule modulates base excision repair. *The EMBO journal*. 28:3207-3215.

Patel, A. G., Sarkaria, J. N. and Kaufmann, S. H. 2011. Nonhomologous end joining drives poly(ADP-ribose) polymerase (PARP) inhibitor lethality in homologous recombination-deficient cells. *Proceedings of the National Academy of Sciences of the United States of America*. 108:3406-3411.

Patel, K. J., Yu, V. P., Lee, H., Corcoran, A., Thistlethwaite, F. C., Evans, M. J., Colledge, W. H., Friedman, L. S., Ponder, B. A. and Venkitaraman, A. R. 1998. Involvement of Brca2 in DNA repair. *Molecular cell*. 1:347-357.

Pearson, G., Robinson, F., Beers Gibson, T., Xu, B. E., Karandikar, M., Berman, K. and Cobb, M. H. 2001. Mitogen-activated protein (MAP) kinase pathways: regulation and physiological functions. *Endocrine reviews*. 22:153-183.

Petermann, E., Orta, M. L., Issaeva, N., Schultz, N. and Helleday, T. 2010. Hydroxyurea-stalled replication forks become progressively inactivated and require two different RAD51-mediated pathways for restart and repair. *Molecular cell*. 37:492-502.

Piazza, A., Boule, J. B., Lopes, J., Mingo, K., Largy, E., Teulade-Fichou, M. P. and Nicolas, A. 2010. Genetic instability triggered by G-quadruplex interacting Phen-DC compounds in *Saccharomyces cerevisiae*. *Nucleic acids research*. 38:4337-4348.

Piccart, M. J., Lamb, H. and Vermorken, J. B. 2001. Current and future potential roles of the platinum drugs in the treatment of ovarian cancer. *Annals of oncology : official journal of the European Society for Medical Oncology / ESMO*. 12:1195-1203.

Rahman, N. and Stratton, M. R. 1998. The genetics of breast cancer susceptibility. *Annual review of genetics*. 32:95-121.

Reedy, M. B., Hang, T., Gallion, H., Arnold, S. and Smith, S. A. 2001. Antisense inhibition of BRCA1 expression and molecular analysis of hereditary tumors indicate that functional inactivation of the p53 DNA damage response pathway is required for BRCA-associated tumorigenesis. *Gynecologic oncology*. 81:441-446.

Ribeyre, C., Lopes, J., Boule, J. B., Piazza, A., Guedin, A., Zakian, V. A., Mergny, J. L. and Nicolas, A. 2009. The yeast Pif1 helicase prevents genomic instability caused by G-quadruplex-forming CEB1 sequences *in vivo*. *PLoS genetics*. 5:e1000475.

Rodriguez, R., Miller, K. M., Forment, J. V., Bradshaw, C. R., Nikan, M., Britton, S., Oelschlaegel, T., Xhemalce, B., Balasubramanian, S. and Jackson, S. P. 2012. Small-molecule-induced DNA damage identifies alternative DNA structures in human genes. *Nature chemical biology*. 8:301-310.

Rodriguez, R., Muller, S., Yeoman, J. A., Trentesaux, C., Riou, J. F. and Balasubramanian, S. 2008. A novel small molecule that alters shelterin integrity and triggers a DNA-damage response at telomeres. *Journal of the American Chemical Society*. 130:15758-15759.

Rogakou, E. P., Boon, C., Redon, C. and Bonner, W. M. 1999. Megabase chromatin domains involved in DNA double-strand breaks in vivo. *The Journal of cell biology*. 146:905-916.

Rottenberg, S., Jaspers, J. E., Kersbergen, A., van der Burg, E., Nygren, A. O., Zander, S. A., Derksen, P. W., de Bruin, M., Zevenhoven, J., Lau, A., Boulter, R., Cranston, A., O'Connor, M. J., Martin, N. M., Borst, P. and Jonkers, J. 2008. High sensitivity of BRCA1-deficient mammary tumors to the PARP inhibitor AZD2281 alone and in combination with platinum drugs. *Proceedings of the National Academy of Sciences of the United States of America*. 105:17079-17084.

Sakai, W., Swisher, E. M., Karlan, B. Y., Agarwal, M. K., Higgins, J., Friedman, C., Villegas, E., Jacquemont, C., Farrugia, D. J., Couch, F. J., Urban, N. and Taniguchi, T. 2008. Secondary mutations as a mechanism of cisplatin resistance in *BRCA2*-mutated cancers. *Nature*. 451:1116-1120.

Sarkies, P., Murat, P., Phillips, L. G., Patel, K. J., Balasubramanian, S. and Sale, J. E. 2012. FANCJ coordinates two pathways that maintain epigenetic stability at G-quadruplex DNA. *Nucleic acids research*. 40:1485-1498.

Sarkies, P., Reams, C., Simpson, L. J. and Sale, J. E. 2010. Epigenetic instability due to defective replication of structured DNA. *Molecular cell*. 40:703-713.

Sartori, A. A., Lukas, C., Coates, J., Mistrik, M., Fu, S., Bartek, J., Baer, R., Lukas, J. and Jackson, S. P. 2007. Human CtIP promotes DNA end resection. *Nature*. 450:509-514.

Segurado, M., Gomez, M. and Antequera, F. 2002. Increased recombination intermediates and homologous integration hot spots at DNA replication origins. *Molecular cell*. 10:907-916.

Shanbhag, N. M., Rafalska-Metcalf, I. U., Balane-Bolivar, C., Janicki, S. M. and Greenberg, R. A. 2010. ATM-dependent chromatin changes silence transcription in *cis* to DNA double-strand breaks. *Cell*. 141:970-981.

Sharan, S. K., Morimatsu, M., Albrecht, U., Lim, D. S., Regel, E., Dinh, C., Sands, A., Eichele, G., Hasty, P. and Bradley, A. 1997. Embryonic lethality and radiation hypersensitivity mediated by Rad51 in mice lacking *Brca2*. *Nature*. 386:804-810.

Shiloh, Y. 2003. ATM and related protein kinases: safeguarding genome integrity. *Nature reviews. Cancer*. 3:155-168.

Shiloh, Y. 2006. The ATM-mediated DNA-damage response: taking shape. *Trends in biochemical sciences*. 31:402-410.

Shiloh, Y. and Ziv, Y. 2013. The ATM protein kinase: regulating the cellular response to genotoxic stress, and more. *Nature reviews. Molecular cell biology*. 14:197-210.

Smith, J. S., Chen, Q., Yatsunyk, L. A., Nicoludis, J. M., Garcia, M. S., Kranaster, R., Balasubramanian, S., Monchaud, D., Teulade-Fichou, M. P., Abramowitz, L., Schultz, D.

C. and Johnson, F. B. 2011. Rudimentary G-quadruplex-based telomere capping in *Saccharomyces cerevisiae*. *Nature structural & molecular biology*. 18:478-485.

Sogo, J. M., Stahl, H., Koller, T. and Knippers, R. 1986. Structure of replicating simian virus 40 minichromosomes. The replication fork, core histone segregation and terminal structures. *Journal of molecular biology*. 189:189-204.

Somyajit, K., Subramanya, S. and Nagaraju, G. 2010. *RAD51C*: a novel cancer susceptibility gene is linked to Fanconi anemia and breast cancer. *Carcinogenesis*. 31:2031-2038.

Sun, H., Karow, J. K., Hickson, I. D. and Maizels, N. 1998. The Bloom's syndrome helicase unwinds G4 DNA. *The Journal of biological chemistry*. 273:27587-27592.

Sung, P. 1994. Catalysis of ATP-dependent homologous DNA pairing and strand exchange by yeast RAD51 protein. *Science*. 265:1241-1243.

Sung, P. and Robberson, D. L. 1995. DNA strand exchange mediated by a RAD51-ssDNA nucleoprotein filament with polarity opposite to that of RecA. *Cell*. 82:453-461.

Suzuki, A., de la Pompa, J. L., Hakem, R., Elia, A., Yoshida, R., Mo, R., Nishina, H., Chuang, T., Wakeham, A., Itie, A., Koo, W., Billia, P., Ho, A., Fukumoto, M., Hui, C. C. and Mak, T. W. 1997. Brca2 is required for embryonic cellular proliferation in the mouse. *Genes & development*. 11:1242-1252.

Szüts, D., Marcus, A. P., Himoto, M., Iwai, S. and Sale, J. E. 2008. REV1 restrains DNA polymerase zeta to ensure frame fidelity during translesion synthesis of UV photoproducts in vivo. *Nucleic acids research*. 36:6767-6780.

Takata, M., Sasaki, M. S., Sonoda, E., Morrison, C., Hashimoto, M., Utsumi, H., Yamaguchi-Iwai, Y., Shinohara, A. and Takeda, S. 1998. Homologous recombination and non-homologous end-joining pathways of DNA double-strand break repair have overlapping roles in the maintenance of chromosomal integrity in vertebrate cells. *The EMBO journal*. 17:5497-5508.

Takebayashi, Y., Pourquier, P., Zimonjic, D. B., Nakayama, K., Emmert, S., Ueda, T., Urasaki, Y., Kanzaki, A., Akiyama, S. I., Popescu, N., Kraemer, K. H. and Pommier, Y. 2001. Antiproliferative activity of ecteinascidin 743 is dependent upon transcription-coupled nucleotide-excision repair. *Nature medicine*. 7:961-966.

Tarsounas, M., Davies, A. A. and West, S. C. 2004. RAD51 localization and activation following DNA damage. *Philosophical transactions of the Royal Society of London. Series B, Biological sciences*. 359:87-93.

Tarsounas, M. and Tijsterman, M. 2013. Genomes and G-quadruplexes: for better or for worse. *Journal of molecular biology*. 425:4782-4789.

Tirkkonen, M., Johannsson, O., Agnarsson, B. A., Olsson, H., Ingvarsson, S., Karhu, R., Tanner, M., Isola, J., Barkardottir, R. B., Borg, A. and Kallioniemi, O. P. 1997. Distinct somatic genetic changes associated with tumor progression in carriers of *BRCA1* and *BRCA2* germ-line mutations. *Cancer research*. 57:1222-1227.

Todd, A. K., Johnston, M. and Neidle, S. 2005. Highly prevalent putative quadruplex sequence motifs in human DNA. *Nucleic acids research*. 33:2901-2907.

Tsang, E. and Carr, A. M. 2008. Replication fork arrest, recombination and the maintenance of ribosomal DNA stability. *DNA repair*. 7:1613-1623.

Tutt, A., Robson, M., Garber, J. E., Domchek, S. M., Audeh, M. W., Weitzel, J. N., Friedlander, M., Arun, B., Loman, N., Schmutzler, R. K., Wardley, A., Mitchell, G., Earl, H., Wickens, M. and Carmichael, J. 2010. Oral poly(ADP-ribose) polymerase inhibitor olaparib in patients with *BRCA1* or *BRCA2* mutations and advanced breast cancer: a proof-of-concept trial. *Lancet*. 376:235-244.

Uringa, E. J., Lisaingo, K., Pickett, H. A., Brind'Amour, J., Rohde, J. H., Zelensky, A., Essers, J. and Lansdorp, P. M. 2012. RTEL1 contributes to DNA replication and repair and telomere maintenance. *Molecular biology of the cell*. 23:2782-2792.

Valerie, K. and Povirk, L. F. 2003. Regulation and mechanisms of mammalian double-strand break repair. *Oncogene*. 22:5792-5812.

Vannier, J. B., Pavicic-Kaltenbrunner, V., Petalcorin, M. I., Ding, H. and Boulton, S. J. 2012. RTEL1 dismantles T loops and counteracts telomeric G4-DNA to maintain telomere integrity. *Cell*. 149:795-806.

Vannier, J. B., Sandhu, S., Petalcorin, M. I., Wu, X., Nabi, Z., Ding, H. and Boulton, S. J. 2013. RTEL1 is a replisome-associated helicase that promotes telomere and genome-wide replication. *Science*. 342:239-242.

Verdun, R. E. and Karlseder, J. 2006. The DNA damage machinery and homologous recombination pathway act consecutively to protect human telomeres. *Cell*. 127:709-720.

Wagner, E. F. and Nebreda, A. R. 2009. Signal integration by JNK and p38 MAPK pathways in cancer development. *Nature reviews. Cancer*. 9:537-549.

Walworth, N. C. and Bernards, R. 1996. *rad*-dependent response of the *chk1*-encoded protein kinase at the DNA damage checkpoint. *Science*. 271:353-356.

Welcsh, P. L. and King, M. C. 2001. *BRCA1* and *BRCA2* and the genetics of breast and ovarian cancer. *Human molecular genetics*. 10:705-713.

Woodward, A. M., Gohler, T., Luciani, M. G., Oehlmann, M., Ge, X., Gartner, A., Jackson, D. A. and Blow, J. J. 2006. Excess Mcm2-7 license dormant origins of replication that can be used under conditions of replicative stress. *The Journal of cell biology*. 173:673-683.

Wu, Y., Shin-ya, K. and Brosh, R. M., Jr. 2008. FANCJ helicase defective in Fanconia anemia and breast cancer unwinds G-quadruplex DNA to defend genomic stability. *Molecular and cellular biology*. 28:4116-4128.

Xia, Z., Dickens, M., Raingeaud, J., Davis, R. J. and Greenberg, M. E. 1995. Opposing effects of ERK and JNK-p38 MAP kinases on apoptosis. *Science*. 270:1326-1331.

Xu, X., Weaver, Z., Linke, S. P., Li, C., Gotay, J., Wang, X. W., Harris, C. C., Ried, T. and Deng, C. X. 1999. Centrosome amplification and a defective G2-M cell cycle checkpoint induce genetic instability in BRCA1 exon 11 isoform-deficient cells. *Molecular cell*. 3:389-395.

Yang, H., Li, Q., Fan, J., Holloman, W. K. and Pavletich, N. P. 2005. The BRCA2 homologue Brh2 nucleates RAD51 filament formation at a dsDNA-ssDNA junction. *Nature*. 433:653-657.

Yu, V. P., Koehler, M., Steinlein, C., Schmid, M., Hanakahi, L. A., van Gool, A. J., West, S. C. and Venkitaraman, A. R. 2000. Gross chromosomal rearrangements and genetic exchange between nonhomologous chromosomes following BRCA2 inactivation. *Genes & development*. 14:1400-1406.

Yujiri, T., Sather, S., Fanger, G. R. and Johnson, G. L. 1998. Role of MEKK1 in cell survival and activation of JNK and ERK pathways defined by targeted gene disruption. *Science*. 282:1911-1914.

Zeman, M. K. and Cimprich, K. A. 2014. Causes and consequences of replication stress. *Nature cell biology*. 16:2-9.

Zimmermann, M. and de Lange, T. 2014. 53BP1: pro choice in DNA repair. *Trends in cell biology*. 24:108-117.

Zou, L. and Elledge, S. J. 2003. Sensing DNA damage through ATRIP recognition of RPA-ssDNA complexes. *Science*. 300:1542-1548.